ALCATEL
SPACE

Planck Optical & RF Verification and Test Plan

H-P-3-ASPI-PL-0137

Product code 221000.

Rédigé par/*Written by*	**Responsabilité-Service-Société** ***Responsibility-Office-Company***	**Date**	**Signature**
Planck PLM Team		12/02/07	
Vérifié par/*Verified by*			
JB. Riti	Planck PLM Technical Manager	14.02.2007	
P. Armand	Planck PLM AIV manager		
T. Banos	Planck PLM Manager	14/02/07	
Approbation/*Approved*			
JM. Reix	H/P Program Deputy Manager	14.02.07	
T. Grassin	Product Assurance Manager	14.02.07	

Entité Emettrice :
(détentrice de l'original) :

ENREGISTREMENT DES EVOLUTIONS / *CHANGE RECORDS*

ISSUE	DATE	§ : DESCRIPTION DES EVOLUTIONS *§ : CHANGE RECORD*	REDACTEUR *AUTHOR*
DRAFT	13/11/01		D. Dubruel
1	15/02/02		D. Dubruel
2	25/06/02	ESA comments taken into account	D. Dubruel
3	09/04/04	ESA comments taken into account & RFQM/FM logic further detailed with optical requirements taken into account	Planck PLM Team
4	17/10/05	§ 4.2.1 :Update of the FM telescope cryo test description according to the new verification approach (videogrammetry test)	JB Riti
		§ 4.2.2 :Update of the FM telescope cryo test description according to the new verification approach (videogrammetry test)	JB Riti
		§ 5.5.1 :Update of the FM telescope cryo test objectives according to the new verification approach (videogrammetry test)	JB Riti
		§ 5.5.2 :Update of the FM telescope cryo facilitie description according to the new verification approach (videogrammetry test)	JB Riti
5	12/02/2207	Reference Document : RD2 and RD4 issue updated §2 : LFI 100 GHz horn removed P20 : OGSE repalced by verification method P22 : Beam ellipticity computation method updated §4.2 : Verification method updated §4.2.3 : FPU alignment process clarified §4.2.4 Characterisation of the FPU updated §4.2.5 Flight performance computation updated §4.3.2 Flight gain degradation computation updated §4.7 Clarification on measured frequencies §5.2.2 Tested frequencies updated §5.3 FM RF test sequence updated §5.5 Telescope FM cryogenic test description updated Annex : diagramm updated	JB Riti

TABLE DES MATIERES / *TABLE OF CONTENTS*

LISTE DES TABLES & FIGURES / *LIST OF TABLES & FIGURES*

1. INTRODUCTION

This document describes the RF verification and test plan proposed by ALCATEL in the frame of the Planck program.

This document reviews all the optical & RF requirements included in the technical specifications (i.e. the SRS & the Planck telescope Optical and RF System Specification).

- For each requirement, the corresponding performance computation is presented. Methods and tools are detailed.
- The verification logic is then introduced: the verification of each performance (by test and/or by analysis) is detailed.

This document also reviews the AIV requirements (as identified in the System AIV requirement Specification) in a similar though more straightforward way (in this case, the proposed implementation of the required measurements is directly explained).

On final, the proposed tests are detailed and the required models are discussed.

Remark: Conversely to previous issues of the present document, the present version addresses both optical & RF requirements.

Applicable documents

[AD1] System Requirements Specification - Document SCI-PT-RS-05991 Issue 3 Revision 2

[AD2] Planck Telescope Optical and RF System Specification - Document n° H-P-3-ASPI-SP-0274 Issue 2 Revision 0 (replacing the former ESA document entitled "Planck telescope Design Specification" and bearing the reference SCI-PT-RS-0724)

[AD3] System AIV Requirements Specification- Document SCI-PT-RS-07430 Issue 2 Revision 1

Reference documents

[RD1] Herschel & Planck Verification Program Plan - Document n° H-P-1-ASPI-PL-0225 Issue 3 Revision 0

[RD2] RFDM Modelling & Analyses - Document n° H-P-3-ASPI-AN-0324 Issue 3 Revision 0

[RD3] Planck Telescope CodeV file - Document n° H-P-3-ASPI-TN-0116 Issue 2 Revision 0 dated 01/04/03

[RD4] Planck PLM Optical Analysis - Document n° H-P-3-ASPI-AN-0331 Issue 2 Revision 0 dated 28/06/02

[RD5] Planck Telescope Optical loadcase definition for optical analysis - Document n° H-P-3-CSAG-AN-2003 Issue 3 Revision 0

[RD6] RFQM Test Requirements - Document n° H-P-3-ASPI-SP-0561 Issue 1 Revision 0

2. PLANCK OPTICAL & RADIO FREQUENCY REQUIREMENTS

In addition to the frequency plan, this section indeed covers two series of requirements:

- the performance requirements (as specified in the SRS and the associated Planck Telescope Optical & RF System Specification - See AD1 & AD2) that must be verified (preferably by test at the higher level possible)

- the verification requirements (characterisation measurements as specified in the Telescope Optical & RF System Specification and the System AIV Requirements - See AD2 & AD3).

Both types of requirements are jointly addressed in order to produce a combined Optical & RF verification & characterisation approach.

2.1 FREQUENCY PLAN

The Planck telescope is a receive-only radio frequency system. The frequency bands of operation are defined around a central frequency imposed by the horns (Annex 3 of AD1):

Frequency (GHz)	30	44	70	100	143	217	353	545	857
Wavelength (mm)	10.0	6.8	4.3	3.0	2.1	1.4	0.8	0.6	0.3

Though not formally specified in the technical specifications, it has been agreed with the instruments teams that the design of the horns defined broad bands by an excursion of +/- 10% around the previous central frequencies. The verification by analysis or test will be carried out within these frequency bands.

2.2 RF PERFORMANCE REQUIREMENTS

2.2.1 Gain degradation (On axis directivity)

The gain degradation performance (P-TEL-PER-035) is specified in AD2 similarly to the WFE and follows an explanation relevant of the theoretical WFE (See section 2.3.1 below that reproduces this explanation). Practically, the definition follows the logic below:

- The on axis theoretical directivity is defined as the reference. It is derived from:
  - the knowledge of the theoretical optical definition of the telescope (defined in AD2),
  - the definition of the horn apodisations (also given in AD2),
  - the definition of the horn locations & orientations (again given in AD2)
  - and the definition of the horn nominal performance in terms of Gain (also given in AD2).
- The telescope performance is then expressed in terms of gain degradation wrt the reference performance derived from the above elements:

P-TEL-PER-035 *The telescope shall achieve a Gain at the horn position of the detectors as defined in* AD 2 *and* AD 3*, at operational conditions and taking into account*

FPU performances as specified in RD 1 *that does not degrade the theoretical value by more than described in* Table 5.2.1-1

Frequency [GHz]	Max reduction in gain [DBi]
30	.5
44	.5
70	.5
100	.5
143	.5
217	1
353	1
545	1.4 tbc
857	2.5 tbc

2.2.2 Beam Ellipticity

The beam ellipticity requirement (P-TEL-PER-040) is expressed in AD2 in terms of deviation (specified at 3 dB below the maximum of each beam):

P-TEL-PER-040 *The ellipticity of the LFI beam pattern is dominated by the optical distortion of the telescope. Inaccuracies due to telescope manufacturing and alignment shall not increase the ellipticity of the LFI beam pattern by more than 1% of the ellipticity given by P-TEL-PER-030 and P-TEL-PER-035 (see note 1).*

Note 1: *If a=major axis, b=minor axis of the best fit ellipse to the 3 dB beam contour, then R=a/b is the ellipticity ratio. The requirement is deltaR/R <=0.01.*

This requirement is linked to the gain degradation performance (See section 2.2.1 above) and to the WFE degradation performance (See section 2.3.1 below).

2.2.3 External Straylight Requirement

The external Straylight requirement (associated to the sources external to the spacecraft in the far-field of the telescope) is defined as the radiative power that reaches a detector within its RF bandwidth and that does originate from sources in the far field of the main beam.

The external Straylight requirement (SPER-060) is defined in AD1 as a rejection in the telescope and spacecraft radiation pattern toward the Sun, the Earth and the Moon. A nota is expressed for the rejection toward the Milky Way (the Milky Way is moving relatively to the overall pattern when the satellite is spun operated):

SPER-060 P	*The system rejection at the detectors for Sun, Earth, Moon at worst case locations shall be , at least :* ***30 GHz :*** *-91 dB , -78 dB and -71 dB respectively.* ***100 GHz (HFI) :*** *-91.5 dB (-99 dB), -78.5 dB (-86 dB) and -71.5 dB (-73 db) respectively* ***353 GHz :*** *-92 dB (-108 dB), -79 dB (-95 dB) and -72 dB (-81 dB) respectively.* ***857 GHz :*** *-98 dB (-122 dB), -85 dB (-109 dB) and -78 dB (-95 dB) respectively.*
Notes	1) The requirement for the Milky Way is of order –65 dB from peak but is driven by the telescope in free-standing configuration. 2) The values between brackets shall be taken as goals .

Remark: There is no explicit dynamic requirement (e.g. for performance computation or tests) in the technical specifications. The dynamic requirements are actually set by the above requirement. In particular, the sizing channel is the 857 GHz channel that asks for a dynamic of 98 dB (with a goal set at 122 dB).

2.2.4 Spacecraft Self Emission Requirement

Another source of straylight is the spacecraft itself. The internal spacecraft sources such as thermal emission from any of the components of the Planck Payload Module and structure generate straylight. These sources propagate the heat to all the spacecraft structural elements. Some radiated power by the spacecraft can reach the detector.

The spacecraft self emission requirement (SPER-065) is expressed in AD1 in terms of Amplitude Spectral Density:

SPER-065 P	*The Amplitude Spectral Density (ASD) at the bolometer (HFI) or cold LNA (LFI) of any signal due to fluctuating thermal emission from a S/C element that couples radiatively into payload detectors , shall be as specified below for each of the five defined individual frequencies , taking into account the power transfer function between the radiating source and the detectors .*

The ASD (in Watts / √Hz) of each frequency component between 0.01 Hz and 100 Hz shall be such that :

Frequency [GHz]	**ASD** [Watt / √Hz]
30	< 3.4 E-18 X
100 (HFI)	< 2.1 E-18 X
353	< 1.8 E-18 X
857	< 2.2 E-17 X

Note :
X is equal to one for any frequency component fo of the fluctuation source synchronous with the Planck S/C spinning rate (i.e. multiple of f.spin = 1 / 60 Hz).

Otherwise , X = (B * t.obs * Delta.f) , where Delta.f = fo – k * f.spin and k is chosen to minimise Delta.f .
t.obs = 3600 * FWHM / 2.5 arcmin , and FWHM is the angular resolution of the antenna radiation pattern in arc minutes .

2.3 OPTICAL PERFORMANCE REQUIREMENTS

2.3.1 WFE degradation

This requirement (P-TEL-PER-030) is defined in AD2 is defined similarly to the gain degradation requirement described above (See section 2.2.1). It follows a detailed explanation presenting what is the theoretical WFE performance wrt which the WFE degradation requirement is expressed:

The WFE requirement on the Planck telescope is defined at a specific set of detector positions (see table) and in a specific way (apodisation).
The exact definition of this parameter, in the following given as WFE, is outlined below:
The WFE has been obtained using apodisation at feed level, while the optical path length difference has been computed in the far field of the antenna. The apodisation in amplitude is used as a weighting function to determine the weighted root mean square of the optical path length difference. The apodisation applied at feed level is gaussian with a 30 dB level in power from the peak at an angle as defined in the table below.

Frequency [GHz]	***Angle 30 dB from Peak [°]***
30 (LFI)	*23.6*
44 (LFI)	*23,6*
70 (LFI)	*21.9*
100 (HFI)	*26.8*
143 (HFI)	*23.7*
217 (HFI)	*21.8*
353 (HFI)	*19.4*
545 (HFI)	*19.4*
857 (HFI)	*19.4*

The telescope achieves with the above definition the theoretical WFE as defined in the following table:
The following table presents, for each horn, the computed theoretical WFE as a fraction of the relevant wavelength.

tit	***lambda [mm]***	***WFE [fraction of lambda]***	***tit***	***lambda [mm]***	***WFE [fraction of lambda]***
|hfi_100_1|	*3*	*0,0237*			
|hfi_100_2|	*3*	*0,0216*			
|hfi_100_3|	*3*	*0,0216*			
|hfi_100_4|	*3*	*0,0237*			
|hfi_143_1|	*2,1*	*0,0298*			
|hfi_143_2|	*2,1*	*0,0210*			
|hfi_143_3|	*2,1*	*0,0207*			

tit	*lambda [mm]*	*WFE [fraction of lambda]*	*tit*	*lambda [mm]*	*WFE [fraction of lambda]*
|hfi_143_4|	*2,1*	*0,0319*			
|hfi_143_5|	*2,1*	*0,0389*			
|hfi_143_6|	*2,1*	*0,0312*			
|hfi_143_7|	*2,1*	*0,0305*			
|hfi_143_8|	*2,1*	*0,0396*			
|hfi_217_1|	*1,38*	*0,0229*			
|hfi_217_2|	*1,38*	*0,0182*			
|hfi_217_3|	*1,38*	*0,0184*			
|hfi_217_4|	*1,38*	*0,0225*			
|hfi_217_5|	*1,38*	*0,0215*	*|LFI_70_1|*	*4,29*	*0,0331*
|hfi_217_6|	*1,38*	*0,0165*	*|LFI_70_2|*	*4,29*	*0,0270*
|hfi_217_7|	*1,38*	*0,0165*	*|LFI_70_3|*	*4,29*	*0,0250*
|hfi_217_8|	*1,38*	*0,0214*	*|LFI_70_4|*	*4,29*	*0,0250*
|HFI_353_1|	*0,85*	*0,0580*	*|LFI_70_5|*	*4,29*	*0,0270*
|HFI_353_2|	*0,85*	*0,0327*	*|LFI_70_6|*	*4,29*	*0,0331*
|HFI_353_3|	*0,85*	*0,0239*	*|LFI_44_1|*	*6,82*	*0,0272*
|HFI_353_4|	*0,85*	*0,0236*	*|LFI_44_2|*	*6,82*	*0,0789*
|HFI_353_5|	*0,85*	*0,0234*	*|LFI_44_3|*	*6,82*	*0,0789*
|HFI_353_6|	*0,85*	*0,0248*	*|LFI_30_1|*	*10*	*0,0234*
|HFI_353_7|	*0,85*	*0,0355*	*|LFI_30_2|*	*10*	*0,0234*
|HFI_353_8|	*0,85*	*0,0580*			
|HFI_545_1|	*0,55*	*0,0975*			
|HFI_545_2|	*0,55*	*0,0564*			
|HFI_545_3|	*0,55*	*0,0609*			
|HFI_545_4|	*0,55*	*0,0980*			
|HFI_857_1|	*0,35*	*0,0640*			
|HFI_857_2|	*0,35*	*0,0606*			
|HFI_857_3|	*0,35*	*0,0603*			
|HFI_857_4|	*0,35*	*0,0674*			

Table 5.2.1-2 - Theoretical telescope WFE

The required telescope performance is defined w.r.t. the theoretical performance.

P-TEL-PER-030 *The telescope shall achieve a WFE at the horn position of the detectors as defined in AD 2 and AD 3, at operational conditions and taking into account FPU performances as specified in RD 1 that does not degrade the theoretical value by more than described in Table 5.2.1-1*

Frequency [GHz]	**Default max contribution**	
	Goal [micron rms]	**Specs.**

30	80	119
44	61	92
70	61	92
100	48	72
143	40	60
217	38	57
353	33	50
545	32	48
857	28	42

Table 5.2.1-3 - WFE maximum degradation

Note: The final WFE = sq root ((max theoretic WFE)^2 + (default max contribution)^2)

2.3.2 Emissivity

This requirement is defined in AD2 (P-TEL-PER-025):

P-TEL-PER-025 *The total emissivity of the telescope optical surfaces over the entire telescope FOV shall be :*

Specification *<6 % EOL*
Goal *<3 % EOL*

Note: This requirement indirectly sets the limit for the telescope transmission (taking account of the reflectors specified emissivity).

2.3.3 Aperture

This requirement is defined in AD1 (SPLA-45):

SPLA-45 *The aperture shall comply with the telescope optical interface requirements as in AD1-3.*

In this requirement, AD1-3 actually refers to the "Telescope Design Specification" now replaced by AD2. Actually, there was no optical interface requirement in this document. The phrase was understood as the theoretical definition of the telescope, which has been maintained/updated in the replacing AD2 specification.

2.3.4 FOV

This requirement is defined in AD1 (SPLA-040) and downlinked in AD2 (P-TEL-PER-020):

P-TEL-PER-020 *The telescope shall have an unobstructed Field of View (FOV) of $\pm 5°$*

The above requirement is linked to the theoretical definition of the telescope also found in AD2.

2.4 VERIFICATION REQUIREMENTS

The following verification requirements also apply:

- In AD2:

P-TEL-VER-052 *The contractor responsible for the telescope shall perform tests on an elegant RF breadboard with the aim of demonstrating the RF properties of the Planck telescope and their correlation with the measurable quantities defined in section 5.5 (in particular P-TEL-PER-030 & 035), and the established optical model for the telescope. These tests shall established beam shapes, straylight and polarisation properties. These tests shall be done with the support of the Instrument teams and the agreement of ESA.*

- In AD3:

Given the criticality for the scientific success of the mission of the optical (radio frequency) properties (e.g. beam shape, polarisation, etc.) of the Planck system, and the fact that the radio frequency properties of the Planck telescope models will only be measured indirectly (using measures such as the WFE), a representative RF model is requested to ensure that the system is performing adequately from the optical/RF point of view.

AIMO-05 *The Planck RF Model shall be used to: (1) validate by measurement the optical and straylight mathematical models used in the design phases, (2) determine by test the radio frequency properties (beam shape and polarisation properties) of the Planck optical system (including detector feed horn, telescope, baffles, shields etc.), (3) establish and verify the relationship between the properties to be measured on the telescope QM and FM (e.g. WFE) and their radio frequency properties.*

Note: As can be seen above (P-TEL-VER-052 in AD2), the verification requirements are explicitly linked to the corresponding performance requirements: P-TEL-PER-030 relates to the WFE degradation requirement while P-TEL-PER-035 relates to the gain degradation requirement.

3. PERFORMANCE COMPUTATION (ANALYSIS)

Prior to be subject to verification, the various specified performances are computed by dedicated analysis. A discussion of the different simulation tools is presented in this section. Then for each performance, the selected method or tool used for its computation is detailed.

3.1 STATUS OF EXISTING TOOLS AND METHODS

The major software tools existing for optical & RF modelling are Code 5 (or Code V), ASAP and Grasp9:

- Code 5 is a well-known optical software used to optimise and analyse all kind of optical systems using a ray tracing method. In particular, this software tool allows to optimise mirrors independently from frequency. It was used during the Planck Payload Architect study to define the Planck telescope optical configuration and is used for the computation of the WFE budgets.

- ASAP has been used in the frame of the Planck Payload Architect Study in order to define the manufacturing tolerances, the integration and the stability of the mirrors and of the structure. ASAP has now been replaced by Code 5 for the sensitivity analysis. It remains a useful tool to analyse straylight sources (it is therefore particularly useful for the assessment of optical test configurations).

- Grasp9 is the well-known RF software developed by the TICRA Company and constitutes the natural reference for the Planck RF analysis.

For information the Planck telescope optimisation involved a combination of the three above software, as follows:

i) Mirrors surfaces shaping aiming at reducing the quadratic sum of the wavefront error (WFE) with a classical optical software: Code 5

ii) Telescope sensitivity analysis with gaussian beam using another optical software: ASAP

iii) Telescope far field radiation pattern computation over the whole space (4π) with actual primary feed diagrams using a classical RF software: Grasp9

In 1999, Alcatel performed a comparative study in the frame of the Planck Payload Architect study. Optical (Code 5 & ASAP) and Radio Frequency (Grasp9) software tools were compared. The methods in use were the Physical Optics (PO) method and/or the ray tracing method.

In particular, a cross validation was performed between Code 5 and Grasp9 for the computation of the main lobes. The figure 4.1-1 displays an example of comparative output.

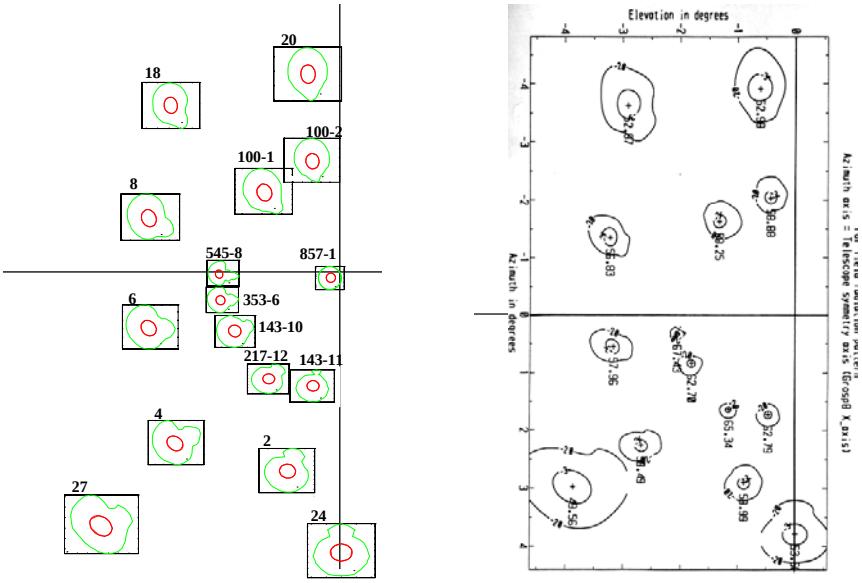

Figure 3.1-1 - Comparison of simulation results with Code 5 (left) & Grasp9 (right) for the non optimised Planck geometry

(*Note*: Drawings not perfectly at the same scale)

First of all, a cross check between Code 5 and Grasp9 for frequencies within the 30 GHz to 353 GHz band shows a nice correlation for the main lobe (see fig 4.1-1 for a comparison of the non optimised telescope at 30GHz). Contour lines plotted at -3 dB and -20 dB below the peak have the same size, shape and orientation. This cross validation shows the validity of both software tools to compute the main lobe.

Compared to Code 5, Grasp9 however provides additional data: the on-axis directivity, the cross-polarisation and the side lobes. Grasp9 also allows to compute the telescope radiation pattern over all directions in space. This is not feasible with Code 5. That explains why Grasp9 was selected to compute the far out side lobes.

Grasp9 allows the computation of far out side lobes thanks to two implemented methods: the physical optics method and the multi-gtd method recently released as an update. The multi-gtd method is convenient for the computation of diagrams for objects including structures and is especially dedicated to high frequency (see TICRA comment in the Minutes of Meeting of the RF expertise clarification & negotiation meeting 12/10/2001 ref H-P-ASPI-MN-457).

In the frame of the Planck programme a RF expertise with the TICRA Company was initiated. This cooperation allowed to ensure the right and best accurate use of Grasp9 in general and of the multi-gtd method in particular. TICRA analysed the numerical method to be used wrt frequency. TICRA also described the computation parameter setting and their frequency dependence law from 30 GHz to 857 GHz for the far out side lobe computation. TICRA also analysed the surface edge shape impact on the diagram.

The Grasp9 accuracy and associated limitation is part of the output of the RF expertise performed by TICRA. As author of the Grasp9 software, TICRA is considered as the only expert company able to perform this kind of analysis. This is even more evident as TICRA was able to modify its source code so as to correct and improve the numerical model when necessary. This ensured a great flexibility in the modelling in order to obtain the best accuracy.

On final the software accuracy and more generally the RF numerical model validation will be taken into account in the verification logic.

3.2 WFE PERFORMANCE COMPUTATION

This section describes the way apodised Wavefront Error is computed. We will first describe the optical model, then the performance. After that we will describe the contributors to performance degradation.

3.2.1 Optical Model

The Optical Model is described in RD3. It is composed of:

- two nominal reflectors at their nominal position
- 63 horns, each one of them having a dedicated parabolic apodisation, as per the specification

A dedicated analysis has been performed in RD4, in order to show that Code 5 is able to accurately compute the impact of apodisation on wavefront error.

3.2.2 Apodised wavefront

The optical quality of the Planck Telescope is specified in terms of Wave Front Error. This is a classical way to specify the ability of an optical imaging system to perform a sharp image. The Wave Front is the surface of equal phase (iso-OPD) produced by a point source. The entrance Wave-Front, coming from cold space, is flat. If the telescope is perfect (i.e. free of aberration) the output wavefront is a sphere, centered on the focal point - this is linked to the fact that all the light "rays" of geometrical optics converge on a single focal point. It gives a perfect "diffraction-limited" image point. However, the actual telescope will not be perfect, because of reflectors distortions and misalignments of the reflectors and FPU and the Wave Front is thus distorted.

For a given ray, the OPD (for Optical Path Difference) is the normal deviation of the actual phase from the ideal one. By hypothesis, the chief ray is considered as a reference and its OPD is set to zero. The root-mean-square value of these differences over the pupil, for a given entrance field angle, is the WFE rms. This can be expressed in wavelength for monochromatic systems. For Planck, due to the large spectral domain covered by the several detectors, it will be expressed in micrometers.

The previous considerations are valid when the following classical hypotheses are made:

- The reference is the perfect optical system (for which WFE rms = 0 μm)
- The intensity distribution is constant over the pupil

For Planck, the previous hypotheses are not verified because, on one hand, the theoretical WFE is not completely negligible and on the other hand, the RF detector taper induces a pupil amplitude apodisation, which has to be taken into account in the WFE computation. These two particular points will be further explained in the next sections

3.2.2.1 Impact of non perfect theoretical optical design.

In the frame of the Planck Architect Study, the optical design of the telescope has been optimized - via the Code 5 optical design software - in order to have a correct image quality over the field of view, taking into account the fact that the farther the detectors are in the field, the higher their working wavelength is. It led to have a better theoretical wavefront in the center than in the field.

The following graph also illustrates this point. It gives the theoretical Wave Front Error in microns for some typical horns:

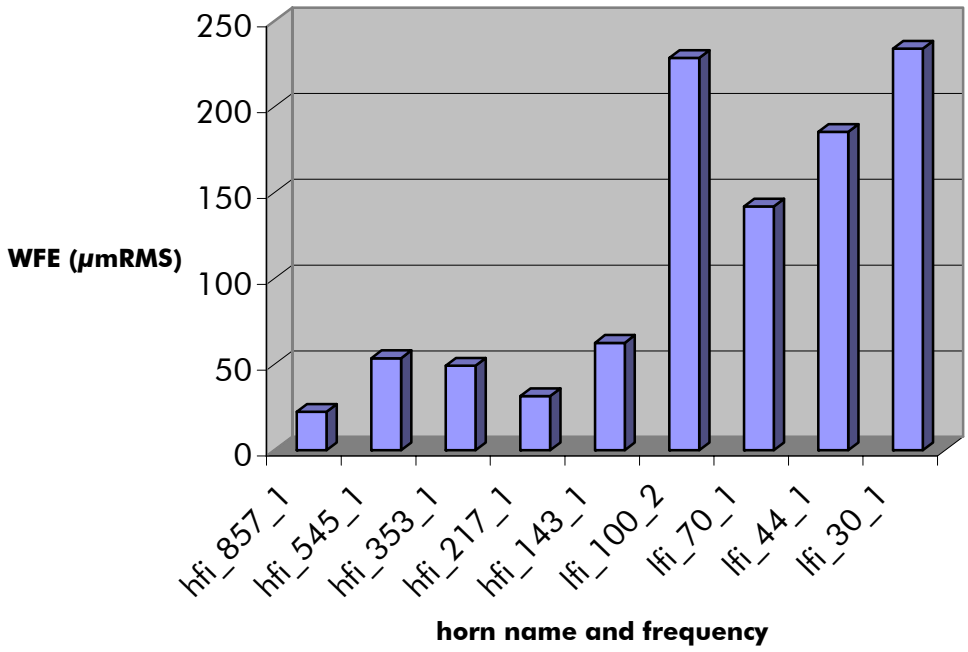

Figure 3.2-1 – Theoretical WFE RMS (in microns) for Typical Horns

To analyze the impact of a perturbation on the optical quality, one has to be able to assess the impact of a small perturbation on a non-perfect wave-front. In that context, the simple usual way to compute WFE, subtracting (RMS or linear) the theoretical WFE from the actual one is not accurate. The proper way to assess the impact of a perturbation on a such a non-perfect system is to subtract wavefronts (i.e. a two dimensional curve) and to compute the RMS value of this "Wavefront Differential".

3.2.3 Contributors to wavefront error

They can be systematically described in the following way:

- reflectors shape:
  - manufacturing
  - environment
  - measurement accuracy
- reflectors co-alignment:
  - structure manufacturing
  - environment
  - measurement accuracy
- PLM:
  - manufacturing
  - environment

In the next paragraphs, an additional type of error is presented: Computation Errors

3.2.4 Computation errors

At each level (reflector, telescope, PLM), computation errors propagate to end in an error in the WFE budget. We can distinguish 2 categories:

- computation accuracy
- model fidelity

These two categories are described in the next sections

3.2.4.1 Computation accuracy

This error is related to the ability of the optical modelling software to compute the Wavefront error , i.e. to subtract two wavefronts. A dedicated analysis has been performed in RD4. It showed that, whatever the aberration, the subtraction of two identical wavefronts - which should give a 0 error - always led to less than 1% WFE, i.e. less than 0.2 μm at 857 GHz, which is fully compatible with the WFE budget.

3.2.4.2 Modelling error

This error relates to the fidelity of the model to the actual hardware design. This error depends on the element (reflector, structure, FPU) and evolves with the development.

3.2.4.2.1 Reflector modelling error

The reflector manufacturer delivered the output from FE Model, which has been best-fitted to feed the optical model (see RD5). The FE model accuracy (10%, agreed with ASED) and the interpolation errors are considered in the budget.

Once the reflectors are tested (optical test in cryo), this error will be cancelled and replaced by the measurement error.

3.2.4.2.2 Structure modelling Error

The modelling errors (E-Modulus, CTE/CME knowledge accuracy, environment knowledge accuracy) are considered in the structure WFE budget (cf. RD5).

The verification method accuracy is also accounted for in the WFE budget.

Most of these errors will be cancelled by the optical cryo test. Only configuration knowledge accuracy, accuracy linked with the extrapolation to in-orbit conditions and measurement accuracy will remain.

3.3 GAIN DEGRADATION & ELLIPTICITY PERFORMANCE COMPUTATION

3.3.1 Gain Degradation

The theoretical gain (on-axis main lobe directivity) corresponds to the response of a telescope perfectly manufactured aligned and cleaned.

The gain degradation comes from:
- reflectors electromagnetic properties: reflectivity, transmittivity, ohmic losses
- surfaces manufacturing errors
- reflectors edge shape
- reflectors thermoelastic distortion, distortion induced by gravity release
- reflectors and focal plane unit misalignment
- reflectors micro-cracks & dust

The proper feed illumination is used. For the analysis, a horn model derived from the detailed feed geometry provided by the scientific team is used in order to obtain the exact detector response.

The first part of the performance computation consists in producing all the theoretical gains for all the detectors at all frequencies (main beam computation in a fine grid and down to –40 dB below maximum). The telescope is considered without any surrounding structure as far as only the main lobe is computed.

The main objective of the degradation computation is then to:
- process the provided reflector electromagnetic property reflectivity, transmittivity, ohmic losses (data provided by the reflectors manufacturer)
- analyse the impact of the surface manufacturing errors
- analyse all the misalignment impacts
- assess by analysis the impact of micro cracks & dust

Each contributor is then quantified.

The main tool available for this analysis is the Grasp9 software using the physical optics method. The physical optics method is perfectly suited for the computation of the main lobe characteristics in a reasonable CPU time. The required inputs for this analysis are:

- the actual focal plane geometry (6 geometrical parameters defining each detector position)
- the detailed inner geometry of each detector
- the phase center position of each detector.

An example computed with Grasp9 for the LFI main lobe computation is provided in figure 4.2-1 using the detector radiation pattern from the PPLA study and the updated focal plane geometry.

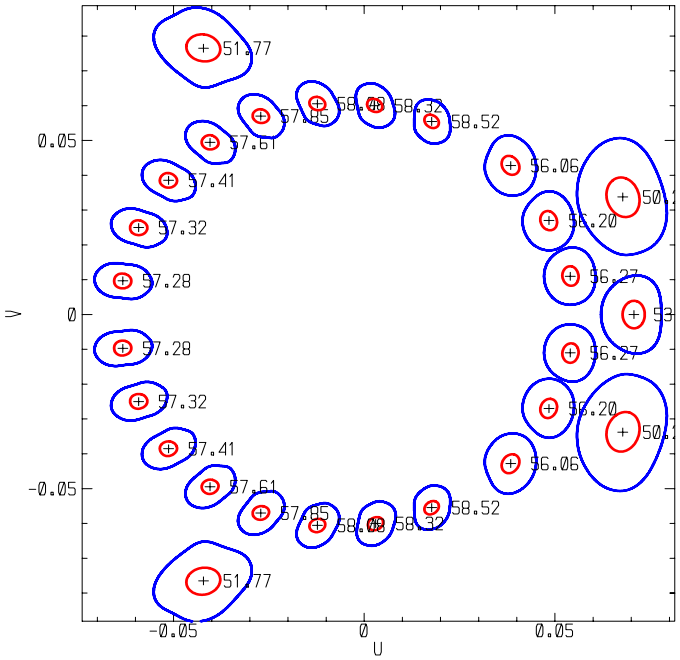

Figure 3.3-1 - LFI patterns - Directivity (dBi)

Note: The numerical values represent the main lobes maximum values. The contour plots correspond to –3 dB and -20 dB below the maximum.

Another example computed with Grasp9 for the HFI main lobe computation is provided in figure 4.2-2 using the available radiation patterns (100 GHz, 143 GHz and 217 GHz frequencies) and the updated focal plane geometry (only 5 parameters available out of 6).

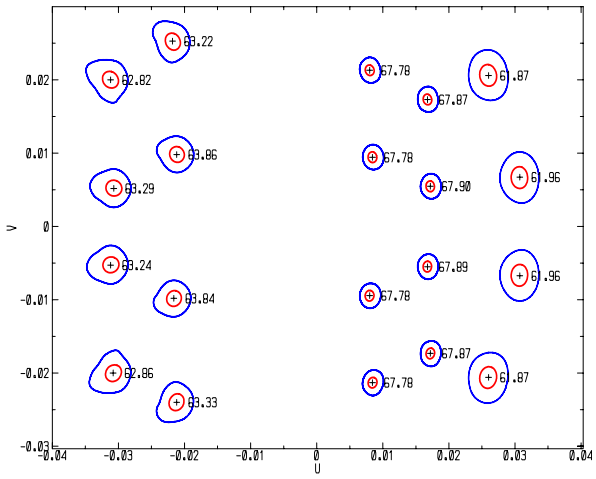

Figure 3.3-2 - HFI 100, 143 and 217 GHz patterns in directivity (dBi)

Note: The numerical values represent the maximum of the main lobes. The contour plots correspond to –3 dB and -20 dB levels below the maximum.

The outputs of this performance computation are:

- the theoretical on-axis directivity
- the performance degradation budgets
- the relative beam pointing in the sky

3.3.2 Ellipticity

Each beam has a nominal (theoretical) ellipticity when the telescope is perfectly manufactured aligned and cleaned. The beam ellipticity deviation is due to the telescope misalignment. It is specified at 3 dB below the maximum for each beam.

The beam ellipticity deviation computation consists in analysing the beam ellipticity for the deterministic case pattern.

3.4 EXTERNAL STRAYLIGHT COMPUTATION

The external straylight requirement is defined as the off-axis rejection in the telescope and spacecraft radiation pattern toward the Sun, the Earth and the Moon (see section 2).

In this frame the corresponding performance computation mainly consists in modelling (with Grasp9) the overall telescope radiation pattern in all directions (See section 3.4.1). However, some effects cannot be directly taken into account in Grasp9 and have to be addressed separately: these are micro-cracks, coatings and dust (See section 3.4.2).

3.4.1 Grasp9 modelling

The radiation pattern is not only the pattern produced by the telescope in freestanding configuration but by the telescope and the surrounding structures (i.e. the whole Planck spacecraft).

The computation therefore becomes more complex: the spacecraft is a set of reflecting and diffracting structures. In addition, the frequency range of operation (30 GHz to 857 GHz) generates an increasing electromagnetic normalised dimension (normalised dimension = actual object size / wavelength) with the frequency.

The only valid electromagnetic computation to solve this problem would consist in using the general theory of diffraction (gtd).

The multi-gtd method was implemented as an add-on package to Grasp9. The difficulty in the use of this software consists for the user in setting the right potential ray combination with the adequate numerical parameters. The use is not straightforward. The TICRA Company was selected to provide a RF expertise in order to implement this method and to compute the 4Pi radiation patterns with the required accuracy.

The external straylight performance computation consists in computing the diagram in spherical cuts around the telescope.

The figure 4.3-1 displays the direction of the different lobes.

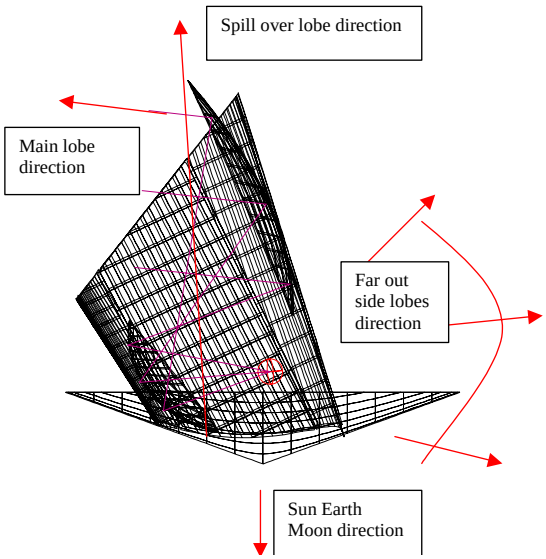

Figure 3.4-1 - Definition of the direction of the main lobes for Planck

The raw output of this analysis is different samplings in cuts over 4 PI for all the frequencies with a reasonable meshing ("reasonable" has to be understood as taking into account CPU time

consumption for the performance computation - the meshing should also be consistent with the tests that are planned). This raw output then allows to derive the rejection performance toward the specified directions.

The required numerical dynamic is 100 dB (with a goal of 125 dB). This dynamic is justified by the requirement in terms of rejection (see requirement SPER-060 in section 2). The most stringent rejection level is specified as -98 dB at 857 GHz (the goal at the same frequency is 122 dB). In order to compare the predicted performance with the requirement the numerical dynamic should have similar or higher requirements.

For the computation of the external straylight performance, the surrounding structure is taken into account in the numerical model. The structure in the RF model is the same structure as the one in the CAD model for the baffle, the grooves, the SVM walls and the solar array. These surfaces are representative from a geometrical point of view: each surface is defined with the same shape and position as the one in the CAD model.

3.4.2 Other contributors (not modelled in Grasp9)

The surface micro-cracks are not in the model nor are coating nor dust. These second-order effects are dealt with separately. A separate study was initiated by ESA with TICRA in order to specifically address micro-cracks. This study has now been completed and a code developed by TICRA and named "Crack.exe version 2.16" has been made available to Alcatel.

In addition, the baffle external surface is composed of a black painted open honeycomb implemented for thermal purposes. This honeycomb is covered with a coating (the black paint) having its own RF properties. Hence an analysis was performed consisting in assessing the geometrical impact of the honeycomb. Then a second analysis was performed consisting in analysing an infinite surface with such a coating. This analysis was performed at all central frequencies for each channel in addition to the upper and lower limit for each channel.

3.5 SPACECRAFT SELF EMISSION PERFORMANCE COMPUTATION

The power reaching one detector is the energy thermally radiated from the structure or diffracted along all the different edges toward this detector.

The straylight signal reaching one detector can be expressed as:

$$SIN_{element}(t) = emissivity_{element} * thermal\_law_{element}(t) * incident\_power_{element}$$

The detailed processing of the above relation is described in the technical note H-P-3-ASPI-TN-0188 dated 24/01/02.

The overall spacecraft self emission is the sum of all elementary straylight laws.

On a practical standpoint, the computation of the spacecraft self emission performance can be split in three phases:

- RF analysis
- Thermal analysis
- Final data post processing (combination of the outputs of the first two phases)

Note: Such a processing however does not rigorously cover all aspects of the Spacecraft self emission performance. The top of the PR can at times be illuminated by the moon, thus inducing a variation law synchronous with the spacecraft spin. The moon illumination then has two consequences:

- The reflector temperature is subject to a tiny thermal fluctuation of its whole surface (the illuminated part first, slowly diffusing towards the bottom of the reflector)
- As the reflector is not perfectly clean once in orbit, the dust directly illuminated by the moon scatters this energy (some of which then follows the optical path towards the horns).

Analyses were implemented during the phase B (See Document referenced H-P-3-ASP-TN-0528) showing that the 2 above effects were indeed negligible compared to the "classical" self emission (the part that is directly linked to the spacecraft self emission).

3.5.1 Spacecraft Self Emission RF performance analysis (first phase)

The RF analysis consists in computing the RF power exchanged between all the spacecraft elements and the detector.

This computation was initiated in the frame of the RF expertise cooperation with the TICRA Company. It started with the selection of the most suited analysis tool: Grasp9. Then the modelling method (multi-gtd or PO) was selected and the adequate model was built. In final, a combination of both modelling methods was retained and specific routines were added to the Grasp9 software in order to avoid some numerical singularities that appeared during the process (See the document referenced H-P-3-ASPI-TN-0323 for a synthesis and the TICRA document referenced S1117-07 for a more detailed assessment).

The output of this analysis was the numerical value of the power exchanged between the various spacecraft structural elements and the detector.

The study evidenced that the thermal paths toward the detector are mainly the following ones:

- diffracted path along structural element edges (e.g. The sorption cooler is thermally varying on its wall; this wall is then “seen” by the detector through successive diffractions along the SVM shield, the 3 grooves, the baffle)
- radiated from the third groove toward the detector
- radiated from the baffle toward the detector
- radiated from the reflectors toward the detector

The Planck Payload Architect study had already shown that the main component of the spacecraft self emission was the energy thermally radiated from the sorption cooler compressor wall and

diffracted along the successive edges. The other sources of self emission were highly damped by the spacecraft itself. This was confirmed by the new run performed by TICRA.

3.5.2 Spacecraft Self Emission thermal performance analysis (second phase)

The thermal analysis consists in determining the temperature cartography and fluctuations of the spacecraft. The required input data is not only the steady state case result, but also the temperature fluctuation laws over time.

Temperature fluctuations are due to the variations of power absorbed by the satellite as well as to the variations of power dissipated by the satellite. The absorbed power variation may be split into two contributions: the first one is the variation of the external environment due to the satellite orbit around the sun and the second one is the satellite absorption variation due to its own attitude on the orbit. Fortunately, an orbit around the L2 Lagrangian point is particularly well suited to minimise temperature fluctuations due to the external environment. Indeed, the planet (including the Earth) and albedo fluxes are negligible.

The only satellite part directly subject to the solar flux is the solar array. The solar array design is as symmetrical (and flat) as possible around the spin axis (except for the areas close to the thrusters, the TMTC antennas…). This design allows to minimise the solar power variation absorbed by the satellite during S/C spinning. Nevertheless a fluctuation level appears when the satellite spin axis is tilted from the sun direction (the worst allowed case being 10 °). This kind of fluctuation at spin rate (60 s period) must be carefully studied.

The main satellite dissipated power variation fluctuations come from the Sorption Cooler with a period of 667 s. The only way to limit its impact is to optimise the components mass, in order to obtain a high specific heat value (thermal inertia) compatible with the mechanical requirements.

The outputs of the thermal analysis are the time dependant thermal laws of all the external spacecraft structural elements.

3.5.3 Spacecraft Self Emission post processing (third phase)

The third step of the analysis consists in computing the overall expression of the spacecraft self emission corresponding to the sum of all elementary laws.

The spacecraft self emission requirement is expressed as an envelope for the Amplitude Spectral Density. Hence the third analysis consists in providing the Fourier transform of the outputs of the first and second analysis.

Note: Rigorously speaking, the satellite geometry (e.g. solar array) and orientation are not perfect. These imperfections were however found to be negligible wrt the issue of self emission. For example, the satellite solar array positioning error is +/-2 mm. This corresponds to an angle of 0.001 mrad, which is not significant wrt the thermal fluctuation and may then be neglected.

4. VERIFICATION LOGIC

The specified optical & RF performances correspond to the operational phase of the Planck spacecraft lifecycle and for the entire operational mission.

Classically, the verification logic relies upon a series of tests achieved on ground with complementary analysis in order to take account of the specific launch & orbital conditions. Among these, one classically finds launch effect, gravity release, radiation & ageing. The spacecraft design usually tends to minimise the corresponding impacts of such environments and the tests performed on ground represent "most" of the in-flight performance.

In the case of Planck, there is in addition a specific situation linked to the cryogenic nature of the payload. This thermal environment, though taken into account in the design, is far from being benign. This is particularly true wrt the thermo-elastic behaviour of the telescope and of the Cryo-Structure. As can be anticipated, it will be impossible to reproduce representative flight conditions for all the test sequences planned on ground (without anticipating too much on the detailed discussion about the verification of each performance, this would require for example RF measurements performed in a cryogenic CATR).

Still, even for the cryogenic tests that will be proposed, the temperature cartography will not be exactly representative of the flight one. Though less important than the complete absence of cryogenic environment, the differences cannot be considered as negligible for large structures requiring high stability, as is the case for Planck.

For the above reasons, the verification approach proposed for some of the optical & RF performances will rely upon models representing the various contributors of the performance budgets (See the discussion about performance computation in the previous section). These models will be validated by one or more major tests performed in a configuration as close as possible from the flight one. The remaining of the contributors and the difference between the test and flight configurations will then be addressed by complementary analysis backed by elementary tests when achievable. This approach, though not commonly used in RF, is quite systematic for large highly stable optical instruments used in space.

4.1 FREQUENCY PLAN

4.1.1 Test frequencies (RF tests)

The frequency bands of operation are defined by an excursion of +/- 10% around the following central frequencies:

Frequency (GHz)	30	44	70	100	143	217	353	545	857
Wavelength (mm)	10.0	6.8	4.3	3.0	2.1	1.4	0.8	0.6	0.3

The proposed RF tests will be performed within these frequency bands.

However, the verification by test cannot be performed at all the frequencies and for all the test models from a technical and programmatic point of view. Below are some further considerations taken into account for the selection of the frequencies for each RF test:

- The 30 GHz is the worst case frequency for diffraction. At this frequency, the diffraction effects are more significant than at higher frequencies.

- The second frequency of interest was initially set at 100 GHz, this frequency being common between the two instruments. This is not the case anymore following the descoping of LFI. However, the 100 GHz channel still keeps a prime interest (e.g. for issues linked with polarisation following the increase in interest for polarisation after the WMAP results).

- The third frequency of interest is 217 GHz, this frequency corresponding to the upper guaranteed frequency of operation for the available and existing European Compact Antenna Test Ranges.

  The available CATR's in Europe are the Alcatel one in Cannes and the Astrium one in Ottobrun. Both CATR's have been manufactured with identical requirements. The CATR upper limit is actually given by the manufacturing quality of the CATR reflectors and by their internal alignment (the large reflectors are manufactured in several pieces).

  However, some recent studies & experiments have shown that these facilities could probably be used for higher frequencies:

  - The Queen Mary Westfield College has demonstrated the possibility to use a CATR well over the guaranteed upper frequency. In that case the measurement possibility was limited to the main lobe only. Side lobes could not be measured.

  - Similar results have been obtained thanks to a recent study (ADMIRALS), this kind of CATR being used far beyond the maximum guaranteed upper frequency.

  Still, the 217 GHz channel remains of specific interest wrt the testing in CATR's due to the additional guarantee that such an intermediate frequency offers.

- 353 GHz is the upper frequency of the single mode detectors.

- The 545 and 857 GHz channels are impacted by the atmospheric propagation attenuation and also due to the multi-mode detector behaviour. At 545 GHz, the atmospheric attenuation due to the air humidity limits RF measurements with regards to dynamic. In addition, the multi-moded propagation in the detector is still not well defined by the HFI team at present time. Some investigations need to be performed so as to definitely clarify the multi-moded propagation.

  However and as evoked above, these frequencies cannot be rejected a priori thanks to the ADMIRALS and Queen Mary Westfield College results (at least for main lobe measurements).

The recent achievements published by Millilab and concerning the use of holographic techniques should also be considered for testing the higher frequencies of Planck.

In final, the idea is to cover all frequencies by at least one RF test (though with the potential exception of the 857 GHz channel and possibly of the 545 GHz channel as well to cope with technical limitations).

4.1.2 RF Test Facilities

The verification by test of RF characteristics requires an adequate test facility. An ESA funded study concerning the test of submillimeter antennas has been conducted by the Queen Mary Westfield College antenna group in 1996 (contract N° 11641/95/NL/PB(SC) dec 96). This study has shown the interest of Compact Antenna Test Ranges.

For the Planck frequencies, the outdoor far field antenna test ranges have to be discarded mainly due to atmospheric attenuation:

frequency (GHz)	Lambda (m)	Far field (m)	Attenuation (dB/km) RH=43%	Attenuation over distance (dB)
30	0.01	450	0.2	0.09
300	0.001	4500	10	45
900	0.0003	15000	100	1500

The above table displays the far field range (2*diameter^2/lambda) of the antenna and the associated atmospheric attenuation. From the significant test range size and the huge attenuation, any outdoor test has to be rejected in view of the required performances.

An outdoor test campaign has been performed by the institute of applied physics (dept of microwave Physics, Bern university). Results have been presented by A Magun and A. Lüdi in AP2000 Davos and confirm the conclusions drawn from the above table. The telescope under study had a 1.5 m aperture diameter and was operating at 212 and 405 GHz. Tests have been performed with an outdoor test range of 7 km. The test report displays results with a limited dynamic of 15 dB below the maximum. This dynamic is not suited for the Planck application where more than 40 dB are required at least for the main lobe and around 100 dB are required for the far out side lobes (See sections below).

For the lower Planck frequencies, CATR's are available and considered adequate. They are preferred to outdoor tests (discarded due to their limited dynamic) or to other types of facilities. The ADMIRALS experience is an example of successful use of a CATR facility at such frequencies: the results of this study will be exploited within the Planck program.

The higher Planck frequencies however set different challenges for CATR's. The recent achievements published by Millilab and concerning the use of holographic techniques may also be considered for testing these higher frequencies.

In the end, the test facility (or combination of facilities) has to be selected upon the main following criteria:

- frequency range of operation
- measurement dynamic
- positioning capability for the test specimen considered

4.2 WFE PERFORMANCE VERIFICATION

4.2.1 General approach

Prior to addressing the verification approach, one should have in mind the Assembly, Integration & Test sequence of the PPLM in general and of the Telescope itself. In practice, one should bear in mind that there are 2 major integration (& test) steps:

- the Telescope: constituted of the Telescope Structure and of the reflectors → It is aligned/characterised by videogrammetry test
- the Telescope Assembly: constituted of the Telescope and of the FPU → the FPU is aligned wrt the Telescope by means of theodolites

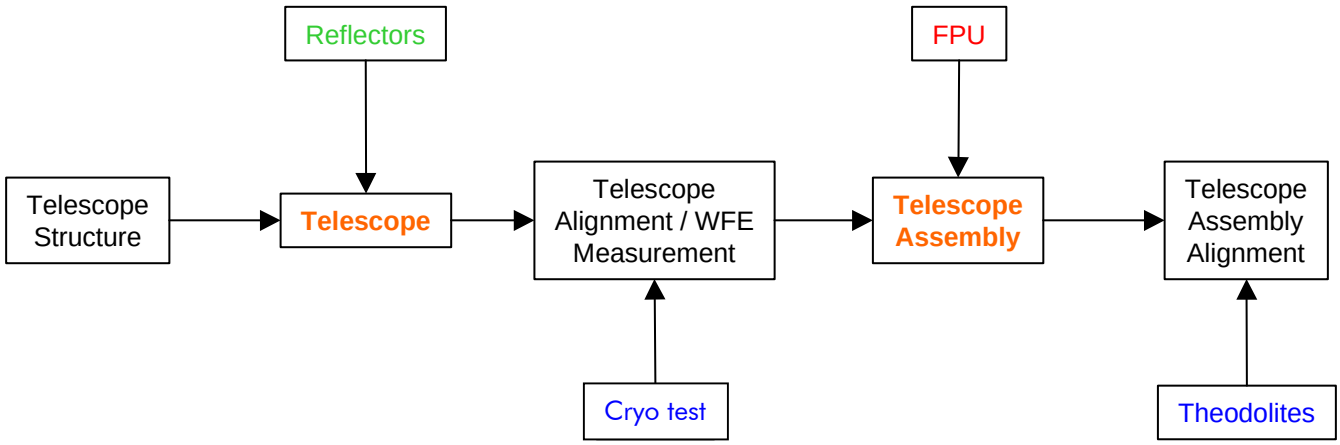

Coming back to verification issues and as explained in the above introduction, the general approach relies upon a performance degradation model backed by a main test performed in a configuration as close as possible to the operational configuration and by additional elementary tests for the contributors that cannot be directly addressed by the main test.

For the WFE performance, the main test used in the verification consists in measuring the Reflector position of the Flight Model under cryogenic environment. As seen in the above diagram, this test is performed at Telescope level. Computation of the Planck WFE performance (including all contributors for the purpose of comparing the achieved performance with the specification) will be achieved through a model that will incorporate in particular the results of the alignment performed at Telescope Assembly level.

In order to reduce these complex alignment/test cryogenic operations, the overall approach relies upon a prediction of the necessary alignment (actually an anti-alignment to compensate for the shrinkage of the structure and of the Reflectors from ambient down to cryogenic temperature).

The reflectors are indeed defocused at ambient so that they might be well positioned (relatively & wrt the FPU) at cryogenic temperature.

This operation first requires a prediction and then a correlation of this prediction:

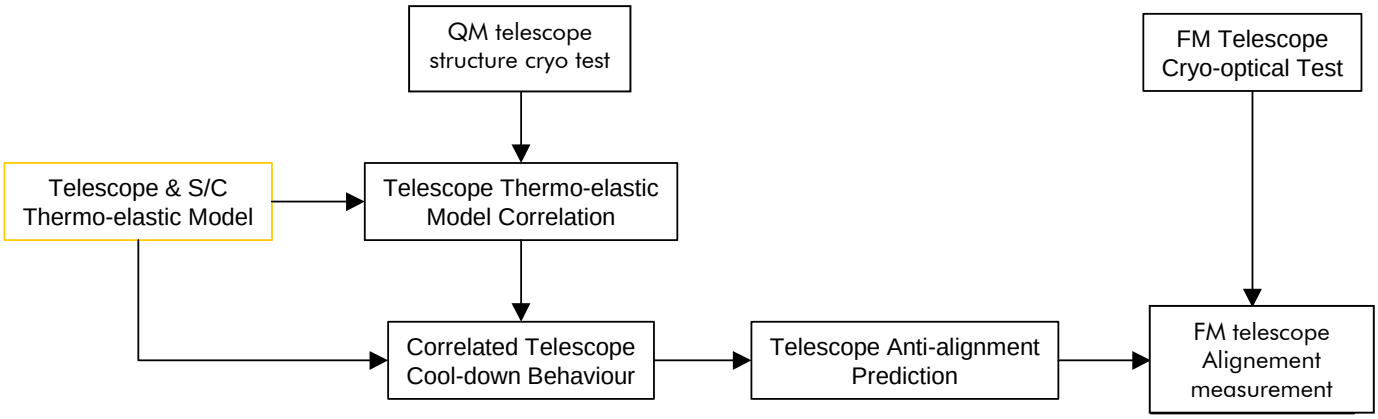

This is achieved in the following way:

- Prediction of the telescope behaviour during cool-down (thermo-elastic modelling including displacements of the interfaces with the Reflectors and the FPU & the interfaces with the cryo-structure)
- Correlation of the thermo-elastic model on the QM telescope model (cryogenic-optical test)
- Anti-alignment of the telescope FM model at ambient (alignment of Reflectors at ambient & compensation of the focus for cryogenic temperature through a displacement of the reflectors)
- Alignment check/ measurement of the FM telescope in cryogenic environment by videogrammetry
- WFE computation

With such an approach, the FM telescope nominally ends up aligned at cryogenic temperature. If the anti-alignment partially fails (residual misalignment superior to what is expected or acceptable), it is always possible to re-align the FM based upon the FM cryogenic test results. This however is time consuming as it requires to re-open the facility, to perform a re-alignment of the Telescope (this time based upon the Telescope FM measurement) and to start a new cryogenic-optical test to characterise the improved alignment.

With the above approach some parameters are not addressed by or are not representative in this main test:

- FPU alignment → only accessible at Telescope Assembly level
- At Reflector & FPU level → See paragraph 4.2.4 below
- All horns → Only some positions (e.g. 5) in the focal plane are directly characterised
- Gravity → The main test is performed with gravity present and not compensated for
- Contamination → The test is performed in a given contamination state which is not exactly the flight one.

- Launch & ageing effects → They have not been experienced by the specimen prior to the test.
- Thermal environment → Though close, the test environment is not 100% representative of the flight environment (different thermal maps and temperature level)

Also, some additional performance parameters are induced by the test itself:

- Anti-alignment accuracy

All of the above needs to be assessed and addressed in the WFE degradation model that comes in complement to the tests.

4.2.2 FM Cryogenic-Optical Test Principle & Limitations

This test will consist in measuring the alignment of the PR, SR and FPU when mounting on the FM telescope structure and cool down to 100K. The measurement method which will be used is the videogrammetry.

4.2.3 Telescope Anti-alignment Prediction & Correlation

The Telescope anti-alignment is predicted via a thermo-elastic model that incorporates the following elements:

- Telescope & Spacecraft (for the I/F) geometry at ambient temperature, measured on various parts (baffle, grooves, solar array, …)
- Reflector properties
- CTE properties over the cool-down temperature range, characterised during the development phase
- Mechanical properties (e.g. E-Modulus), also characterised over the cool-down temperature range during the development phase
- Temperature maps in operational conditions (in-orbit)

Note: the FPU is not compensated during the anti-alignment process but by shimming at telescope FPU I/F, after the FM cryo test.

The parameters involved in the prediction of the anti-alignment and listed above are subject to correlation at various levels:

- CTE properties are characterised at material level: not all materials are known with a sufficient accuracy down to cryogenic temperature. This is particularly true for composites (GFRP, CFRP). In addition, CTE homogeneity is addressed via measurements during the manufacturing process of the composites.
- Mechanical properties are also characterised at material level (for similar reasons as for CTE).
- Temperature maps are obtained through a model: the maps are indeed derived from a thermal model, which is in turn correlated by the CQM-T Vacuum test PMF2 cryo test.
- Finally, the overall thermo-elastic model is also correlated through a dedicated test on the QM. The test is performed at Telescope structure level with representative interfaces so as to

take account of the effects induced by the rest of the spacecraft (i.e. the SVM & the Cryo-Structure).

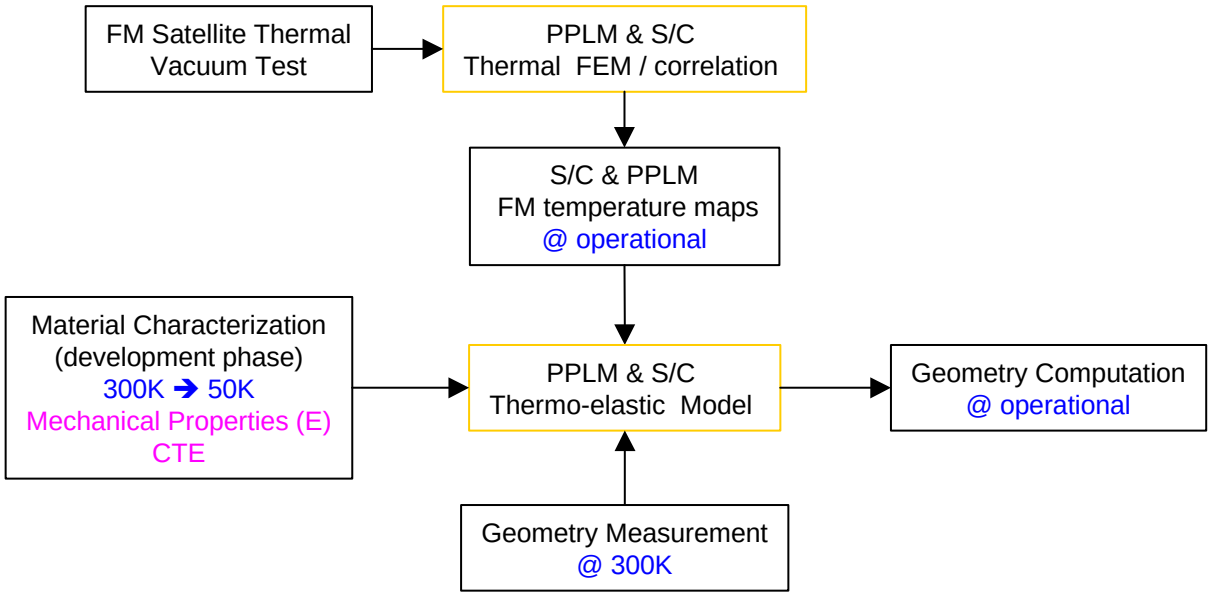

Note: The thermal model allows to derive the in-orbit geometry of all the PPLM elements (and not only of the Telescope), which is needed for RF performance computation. Similarly, this model also provides the prediction of in-orbit temperature fluctuations, which is needed for straylight (Spacecraft Self Emission) computation.

In practice, the situation is a bit more complex than the straightforward process described above. It was decided for programmatic reasons to perform the QM cryo-optical test not at CSL as originally planned but at Alcatel. This had for consequence to limit the achievable temperature to around 100 K, thus creating a difference between the correlation configuration on the QM (around 100 K) and the FM alignment configuration (around 40 K). This difference induces the need to extrapolate the correlation performed on the QM down to the temperature of the FM test. This in turn induces an additional inaccuracy that needs to be taken into account.

The overall QM/FM prediction/correlation/extrapolation/alignment/WFE computation process is tentatively detailed in the diagram below:

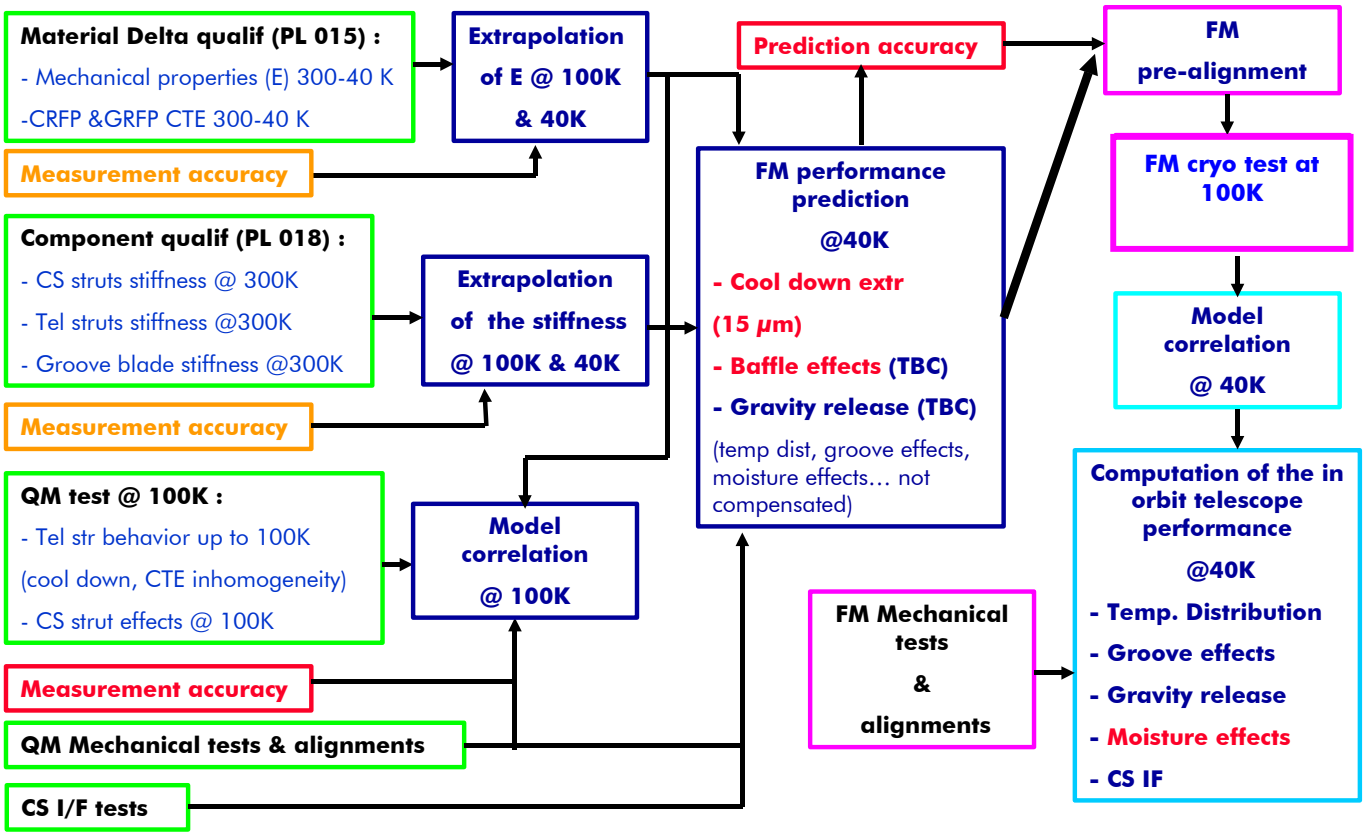

4.2.4 Characterisations needed at Reflector & FPU Level

The Reflectors and the FPU are first specified in terms of performances at operational temperature. These include:

- the theoretical performance at ambient
- the deformations induced by cool-down (for the FPU, this covers the internal FPU alignment – LFI-to-HFI & horn-to-horn – as well as the change in dimensions of each horn)
- the displacements (translations & rotations) wrt the defined interfaces
- the launch & ageing effects

In addition, Reflectors & FPU are also specified in terms of performance degradation associated to the effects linked with the interface deformations (induced by the behaviour of the telescope).

As can be seen, the above specifications are consistent with the limitations of the Telescope cryo-optical test mentioned above. In terms of verification, all the contributors included in these specifications have to be addressed (i.e. characterised) at the corresponding reflector/FPU level. This implies:

- For the Reflectors:

- a characterisation of the WFE at ambient and at cryogenic temperature, including small scale features of the reflector surface (to complement the Telescope data derived from the Telescope FM cryo-optical test)
- a characterisation of the Best-Fit-Ellipsoid (knowledge of the shape - i.e. radius & conic constant - & of the position - i.e. translations & rotations -) at ambient and at operational temperature wrt the defined interfaces
- a characterisation of the effects induced by a deformation of the interfaces (WFE degradation, change in shape & position of the BFE)

As shown on the diagram below, this set of data is used either for the Telescope alignment process or directly in the WFE degradation model:

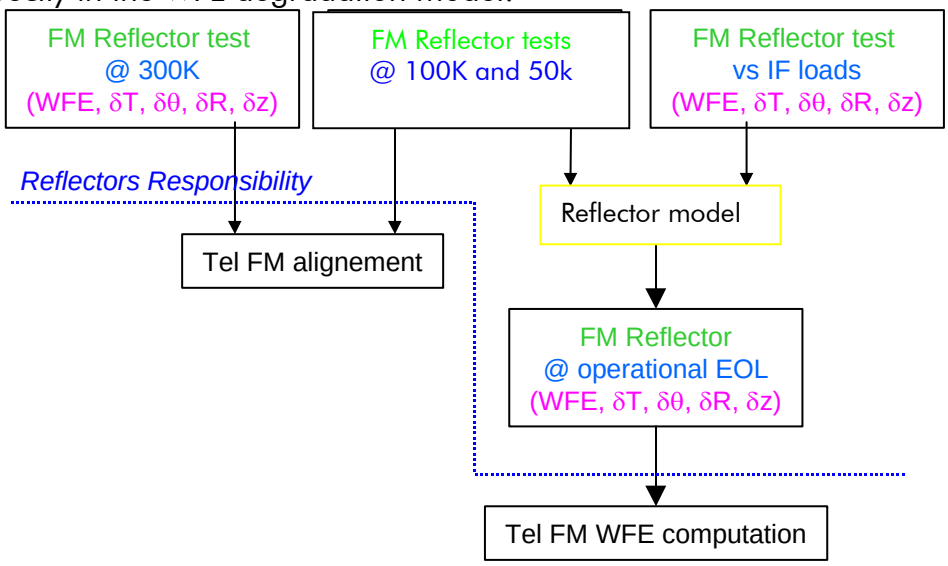

Note1: The following abbreviations are used for the diagram above and for the similar ones displayed in the following pages: δT covers the translations of the corresponding element; δΘ is for the rotations, δR for the radius and δz for the conic constant.
Note2: For the computation of the Telescope FM WFE, the useful parameter is the set of characteristics associated with the Reflectors under the proper in-flight environments (and all over the spacecraft lifetime → EOL is considered as a worst case). As for the Telescope, this is not directly obtained by the tests performed (different thermal maps, …). The operational performance has indeed to be derived from the Reflector tests through a specific FEM.

- For the FPU:
  - The knowledge of the horn beam characteristics at operational temperature (including the horn taper used for the computation of the apodised WFE) including all internal FPU effects (e.g. LFI-to-HFI & horn-to-horn misalignments)
    Note: It is not planned to measure the horn pattern at cryogenic temperature. These characteristics are actually derived from the knowledge of the horn geometry (including all serrations). However, the horn geometry will not be measured at cryogenic temperature. This will indeed be derived from a measurement of the geometry at ambient associated to a thermo-elastic model to take account of the cool-down effect (change in frequency,

displacement of the phase centre wrt the horn interface and scaling effect on the horn internal geometry).

- The characterisation of the displacements (rotations & translations) of the FPU wrt its interfaces between ambient & cool-down
- The characterisation of the effects induced by a deformation of the interfaces (change in position - translations & rotations - of the horns).

As the FPU is not part of the Telescope FM cryo-optical test, this set of data is not taken into account for the Telescope alignment and is only fed into the WFE degradation model:

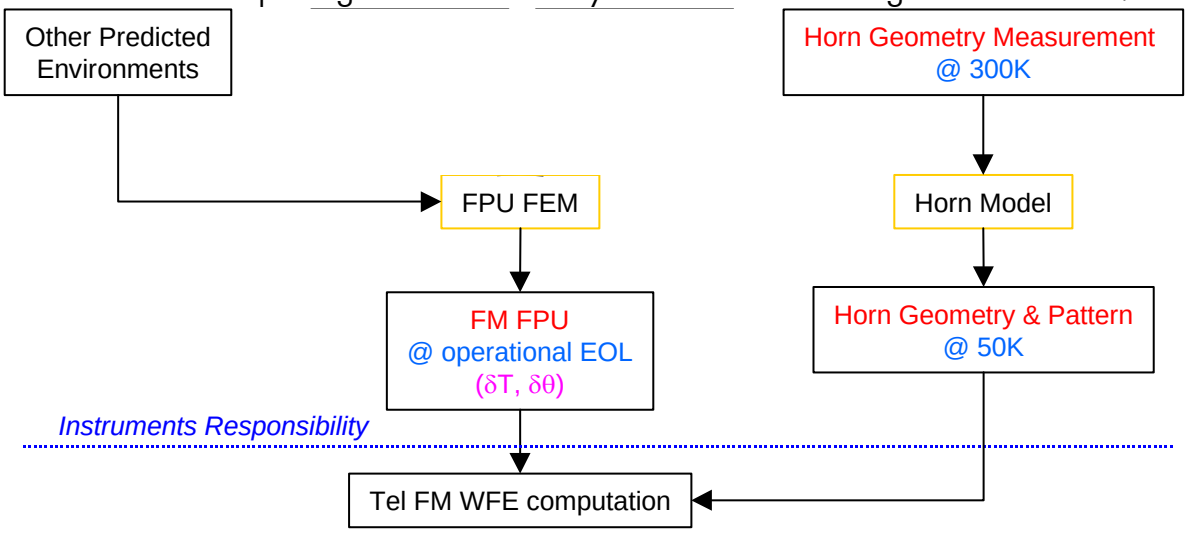

Note: As in the case of the Reflectors, the operational (EOL) FPU performance has to be derived from the tests through a specific FEM prior to being used for the computation of the Telescope WFE.

In both cases (Reflectors & FPU), launch & ageing effects need to be taken into account by analysis. Contamination is addressed by analysis as well but globally at System level (and only for the performances that are impacted by it: i.e. performances linked with transmission & far out side lobes).

4.2.5 In-flight Performance Computation

Relying upon the tests and analysis performed at various levels, the Telescope WFE performance is finally computed via a performance model built around an optical model implemented in the Code 5 software. This computation incorporates the main four performance verification bricks discussed in the above paragraphs:

1. The Telescope FM cryo-optical test (alignment measurement at 100K by videogrammetry measurement)
2. The FPU alignment test
3. The knowledge of the FPU
4. The knowledge of the Reflectors (backed by dedicated cryogenic tests)

The computation of in-flight performances also incorporates the contributors not already covered by these four main bricks: launch & ageing, interface deformations induced by the Cryo-Structure, …

Note1: As for the Reflectors & the FPU, the results of the Telescope FM cryo-optical test are not directly incorporated into the WFE computation model so as to take account of the differences between the test & in-flight configuration. Here also, a FEM is used to perform the extrapolation between these two configurations.
Note2: Bricks 1 and 4 are partially redundant as the Reflectors are mounted on the Telescope during the Telescope FM cryo-optical test. However, this test alone is not sufficient as explained above (e.g. does not cover reflector surface small features nor test to in-flight extrapolation of the reflectors). Redundant information will be addressed in the Code 5 WFE Model (via Zernike polynomials or surface map, up to the spatial order for which the redundancy for large scale features exists).

4.2.6 WFE Verification Synthesis

The diagram below provides a summary of the overall WFE performance verification approach:

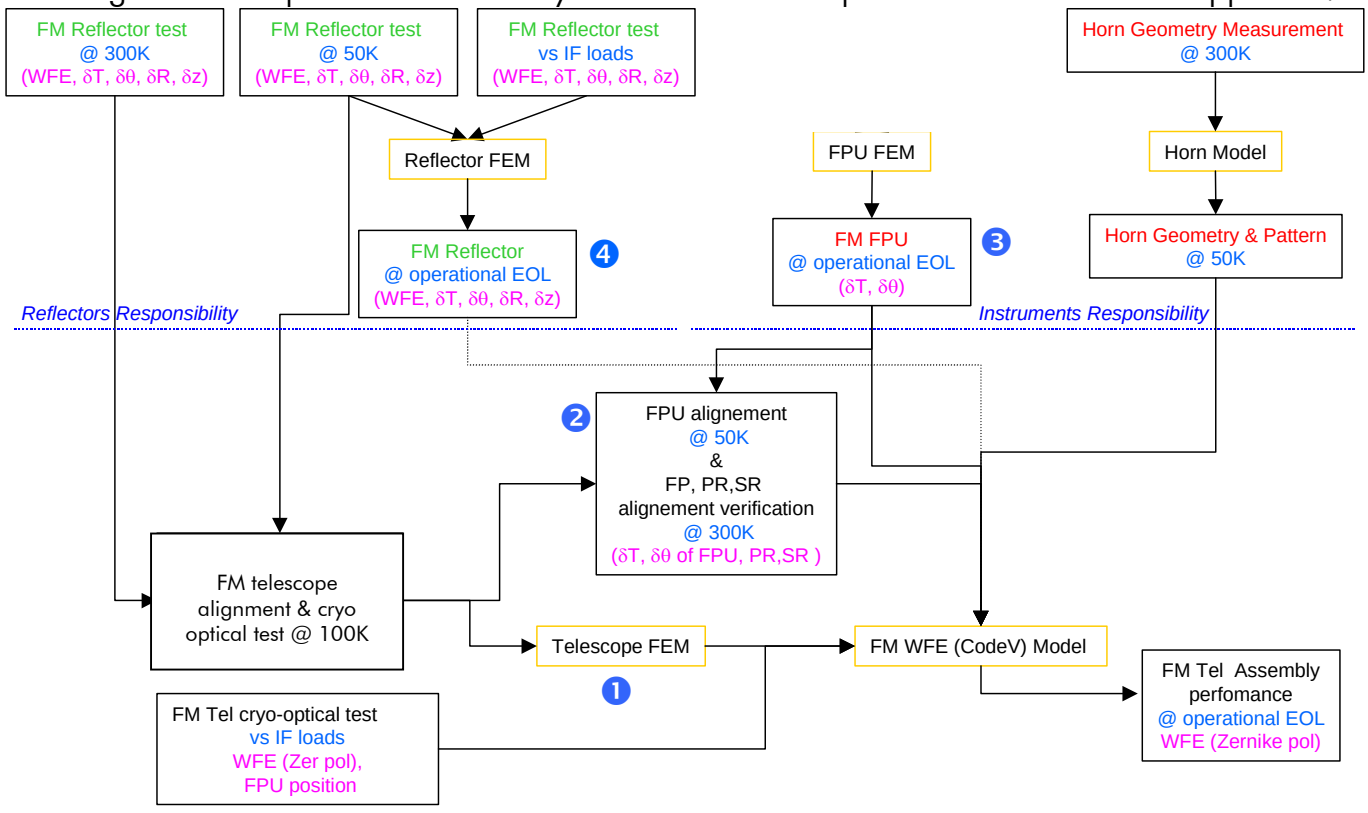

4.3 GAIN DEGRADATION & ELLIPTICITY PERFORMANCE VERIFICATION

4.3.1 General Approach for Gain Degradation Verification

The gain degradation (or maximum directivity degradation) comes from to same causes that also cause the WFE degradation:

- the Telescope structure (stability/distortions, cool-down behaviour),
- the Reflectors (electromagnetic properties - reflectivity, transmittivity & ohmic losses -, surface shape & associated manufacturing errors, micro-cracks, stability/distortions, cool-down behaviour)
- the FPU (horn patterns, internal alignments, stability/distortions, cool-down behaviour)
- the alignments (Reflectors & FPU) & associated compensation (anti-alignment to compensate for cool-down effects on focus at Telescope level)
- the test configurations (difference between test & in-flight configurations, accuracy)
- the other contributors (launch & ageing effects, …)

The verification approach is therefore similar except that RF measurements replace WFE measurements for the main test backing the performance verification.

The RF characterisation approach is based upon the fact that a main lobe known down to 40 dB below the maximum allows the computation of the gain through integration of the pattern (See section 3). The gain degradation is then derived by comparison with the theoretical value: the theoretical on-axis main lobe directivity corresponds to the response of a telescope perfectly manufactured, aligned and cleaned (this value cannot be directly measured, as the specimen under test will inevitably include some imperfections).

Note: The error obtained after the integration process is lower than the measurement uncertainty. That explains why 40 dB are sufficient to obtain the on-axis gain. The main condition associated to this result is that nowhere else in the diagram exists a lobe higher than (max-40 dB).

Measuring the main lobe actually requires measuring the following data:

- the main lobe shape down to –40 dB with a measurement accuracy imposed by the integration process
- the main lobe position (in the sky) relatively to the telescope axis.

The measured main lobe includes the reflector electromagnetic properties, the surface manufacturing errors and the micro-cracks (if any). The measurement also includes the misalignments corresponding to the test configuration (see also the discussion about theoretical, test and actual misalignment cases and induced performance budgets in section 3). The on-axis theoretical directivity is obtained through a pattern post processing.

4.3.2 In-flight Gain Degradation Performance Computation

As for WFE, the in-flight performances will be derived from a computation relying upon a RF model (this time implemented in the Grasp9 software replacing the Code 5 software used for WFE). This computation will incorporate the same main four performance verification bricks discussed in the previous section related to WFE performance verification:

1. The Telescope FM cryo-optical test (alignment measurement at 100K by videogrammetry)
2. The FPU alignment test
3. The knowledge of the FPU
4. The knowledge of the Reflectors (also backed by dedicated cryogenic tests)

The computation of in-flight performances will also incorporate the contributors not already covered by these four main bricks: launch & ageing, interface deformations induced by the Cryo-Structure, …

Alignments measured during the Telescope FM test will be used as input for this model as will be the alignments issued of the FPU alignment process. The differences between the test and flight configurations (including differences in alignments and other perturbations) will be identified and the flight performances will be computed based on the derived model correlated by the tests and extrapolated to the flight configuration (same approach as for the computation of the WFE flight performance).

The overall model architecture and computation process will be in all points identical to its counterpart used for WFE:

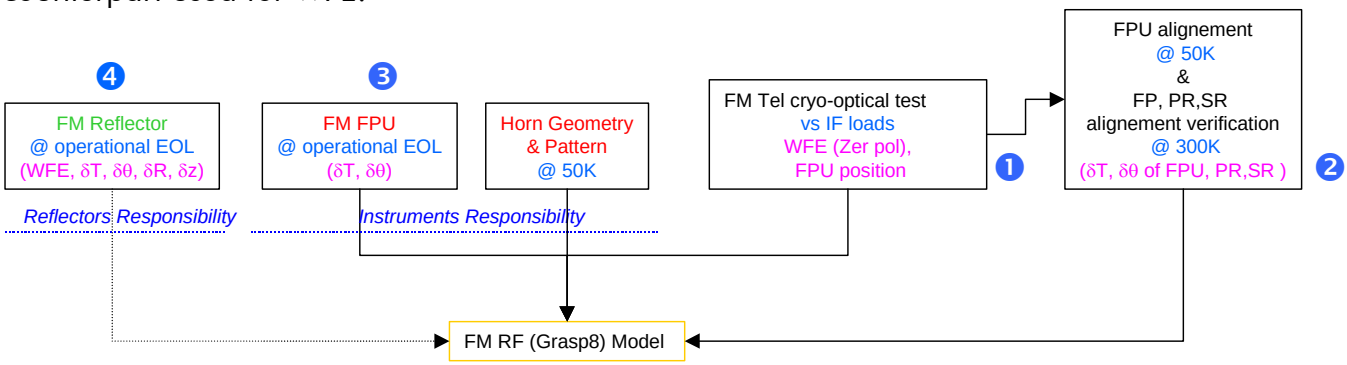

The verification process could indeed stop there if the main test backing the computation of the gain degradation in-flight performance was performed on the FM (as is the case for WFE). This however is not the approach selected as a dedicated model called the RFQM is planned for that purpose (as well as for all the other RF performances).

Here again, with the introduction of a specific test model different from the flight model comes the need for a second major step in the verification process linked with the extrapolation between them and hence with the correlation of the RF models (two Grasp9 models will be defined: one for the RFQM for correlation purposes and another one for the FM to compute the in-flight performances).

The previous diagram therefore needs to be completed in the following way so as to take account of this RF model correlation/extrapolation process:

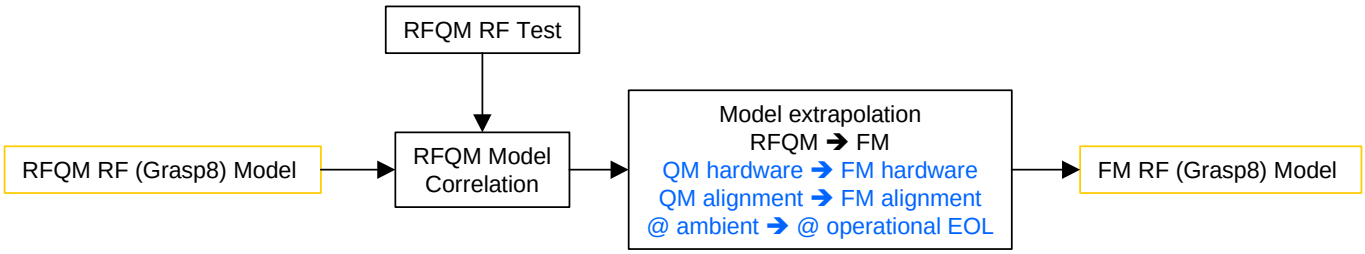

4.3.3 Impacts of the RF Model Correlation process onto the RFQM

Due to correlation objectives and as the FM, the RFQM needs to be optically aligned with the optical parameters (WFE & alignment) being transferred to the RFQM RF (Grasp9) model. The approach is similar to the approach selected for the FM. As for the FM, it also relies upon reflectors & FPU data for both the alignment process and the optical (and RF) performance prediction models.

Apart from manufacturing differences (at Telescope, Reflectors or FPU level), the only other difference lies with the alignment approach. As the RFQM is only required for RF tests (performed at ambient), it does not need to be aligned for a cryogenic environment. Analyses have shown that the Planck Telescope aligned at ambient and operated at ambient had very close performances when compared to the same Telescope operated at cryogenic temperature after implementation of an anti-alignment procedure (to compensate for the effects of the cool-down onto the focus, as is the case for the FM). In other words, the difference is small enough so as to be easy to extrapolate with sufficient accuracy.

The above approach (alignment at ambient / operation at ambient / no anti-alignment) was selected for the RFQM. Apart from that, the overall RFQM alignment/performance measurement/model correlation then follows the FM approach. It relies on the various levels of characterisations performed at Reflectors, FPU and Telescope levels (theodolite measurements).

The first difference comes from the fact that these characterisations now concern the QM hardware that constitutes the RFQM. The second difference takes account of the fact that the RFQM is only operated at ambient. QM Reflector & FPU characterisations performed at ambient are used for optical alignment & for the RF model (where the FM logic also has to incorporate the cool-down effects). This also reduces the need for FEM's (no need to take account of the difference in test configurations such as temperature maps as all operations & characterisations happen in a simple & common ambient environment).

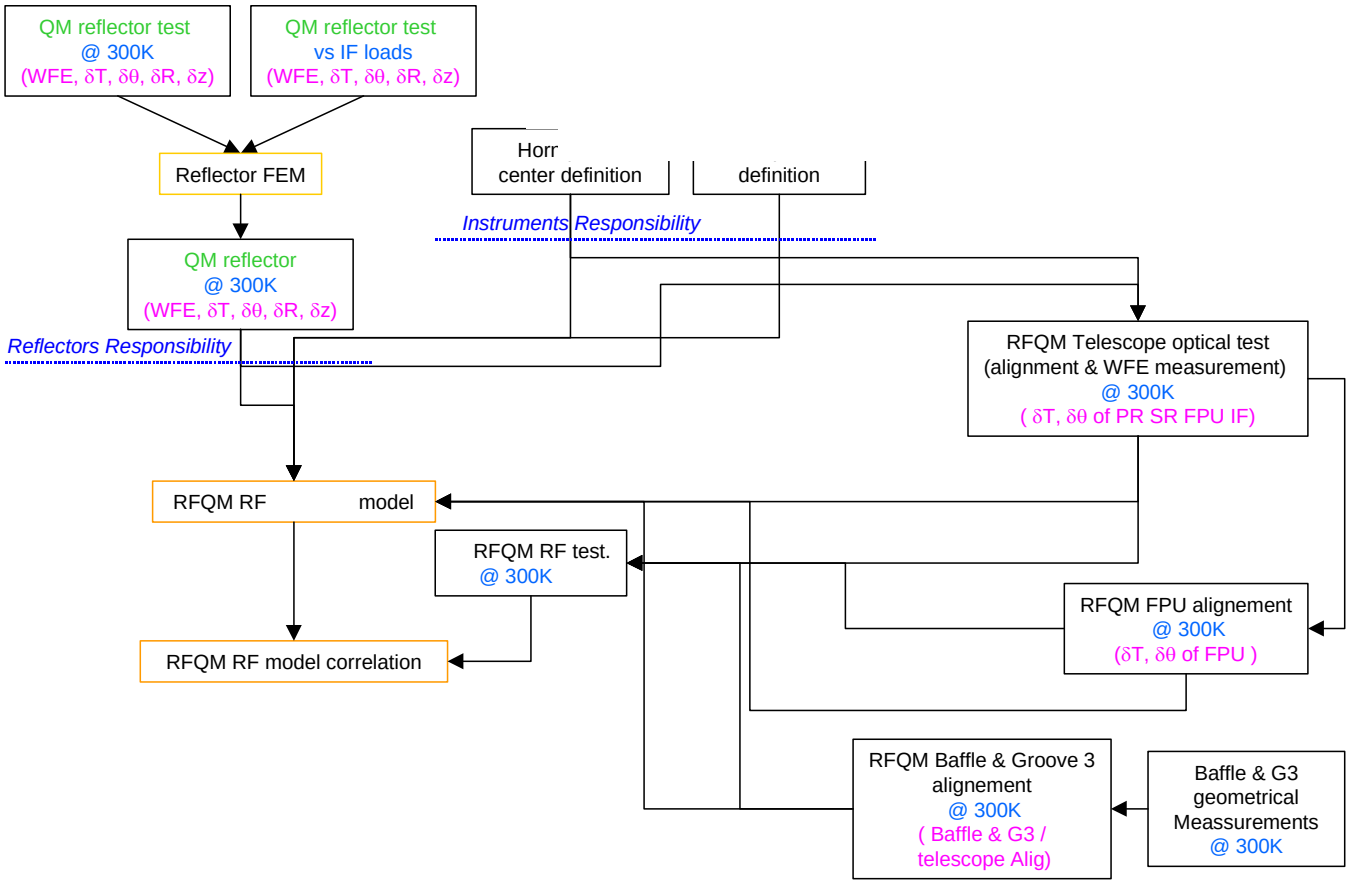

Note: Limiting ourselves to the correlation of the gain degradation model, the Baffle & Groove 3 could be deleted from the above figure as they have little or no influence on the gain degradation performance (as for WFE performance verification). However they play a role in the side lobe characteristics, which is another objective for the RFQM test (see below) and have therefore been kept in the above diagram.

4.3.4 Ellipticity Performance Verification

Each beam has a nominal ellipticity when the telescope is perfectly manufactured, aligned and cleaned. The beam ellipticity deviation (specified at 3 dB below the maximum for each beam) comes from the telescope misalignments.

The proposed verification approach follows in all points the one proposed for the verification of the gain degradation performance: patterns of the main lobes are acquired and correlated with a Grasp9 RF model representing the test configuration (RFQM). The Ellipticity degradation performance is then derived while the RF model is correlated for the test configuration (RFQM). The correlated model is then extrapolated for the FM and to in-flight conditions taking account of the differences between the test (RFQM) and flight (FM) configurations. The computation of in-flight performances also includes additional data coming from the Reflectors and the FPU as well as the usual other contributors (launch & ageing, …).

4.4 EXTERNAL STRAYLIGHT PERFORMANCE VERIFICATION

The external straylight induced noise requirement is defined as a rejection in the telescope and spacecraft radiation pattern toward the Sun, the Earth and the Moon (see section 3.2). In this frame, the verification requires to check the satellite radiation pattern in the directions where the Sun, the Earth and the Moon (later called "the planets" for simplification purposes) are located (i.e. a cone of 32° centred on the satellite spin axis and in the opposite direction from the baffle entrance - See the figure below).

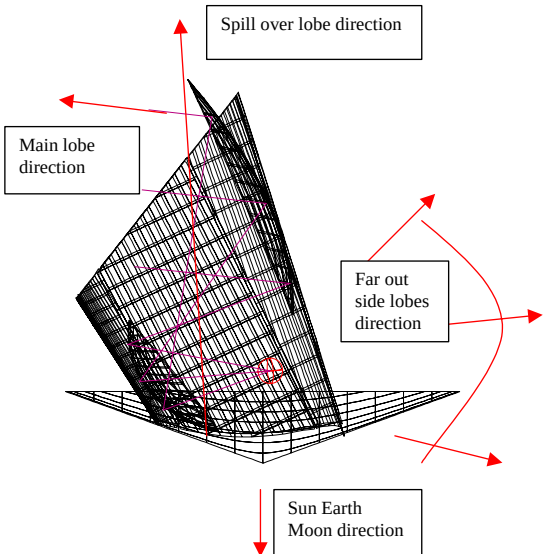

Figure 4.4-1 - Definition of the direction of the main lobes for Planck

For practical reasons, it is not feasible to provide a fine two-dimensional meshing of any extended area of the pattern. The verification consists in obtaining the diagram in spherical cuts around the telescope with an adequate meshing.

The adequate meshing has to be defined taking into account operational constraints (acquisition time per cut), the CPU time consumption for the analysis and the verification requirements (See section 4.7 below).

The standard sampling formula used for antenna measurement is:

Delta = arcsin (lambda/(4*Dant))

with: lambda = wavelength

and Dant =antenna diameter.

This formula defines the angular step between two acquisition points. It is usually considered to provide a sufficient pattern sampling: the patterns obtained with such a sampling are nicely reproduced and can be compared to computation. The table below declines this formula for the various Planck frequencies:

Frequency (GHz)	30	44	70	100	143	217	353	535	857
Wavelength (mm)	10.0	6.8	4.3	3.0	2.1	1.4	0.8	0.6	0.3
Dant (mm)	1500	1500	1500	1500	1500	1500	1500	1500	1500
lambda/(4*Dant)	0.001665	0.001135	0.000714	0.000499	0.000349	0.000230	0.000141	0.000093	0.000058
Angular step : Arcsin(lambda/(4*Dant)) (degrees)	0.095396	0.065043	0.040884	0.028619	0.020013	0.013188	0.008107	0.005349	0.003339
Number of points in a 360° cut	3773	5534	8805	12579	17988	27296	44404	67298	107803
Number of phi cuts	1886	2767	4402	6289	8994	13648	22202	33649	53901
Total number of points	7115878	15312578	38759610	79109331	1.62E+08	3.73E+08	9.86E+08	2.26E+09	5.81E+09

Table 4.4-2 - Standard sampling formula declination

Based upon this table and following various exchanges with the scientists during the Telescope Working Group meetings, the following meshing was agreed for the verification of the rejection performance (in the direction of the planets):

- a meshing (in theta) of 0.5°
- a meshing (in phi) corresponding to an angular step of 5° or 10°

The dynamic measurement range has to be as close as possible to 100 dB. This dynamic is justified by the rejection requirement (requirement SPER-060 in AD1 → See section 2). The largest specified rejection is 98 dB at 857 GHz (The goal at the same frequency is 122 dB). In order to compare the predicted performance with the tests, the dynamic of the numerical model must be at least equal.

The tests associated to the verification of the rejection performance are mainly performed on a representative dedicated model: the RFQM. Prior to this model, an early model (the RFDM) will be used to validate that such a high dynamic as the one required by the verification of the rejection performance is achievable (at least at some frequencies).

In addition to the tests, modelling and analyses are carried out to extrapolate the results obtained on ground with the RFQM to the performances of the FM satellite in flight configuration. As for gain or ellipticity, the following parameters are taken into account for this extrapolation:

- difference in reflector performances
- difference in alignment (use of alignment results coming from the FM cryo-optical test)

For the computation of side lobes, the spacecraft geometry under operational conditions is also important. In order to address this, the following is implemented:

- A thermo-elastic model of the telescope and of the rest of the Planck Spacecraft (to address the telescope interfaces) is built. This model is fed by the measured geometry of the spacecraft elements at ambient (e.g. baffle, grooves, solar array), of the material behaviour from ambient down to cryogenic temperature (e.g. CTE; E-modulus) and of the predicted temperature cartography of the spacecraft while in-orbit.

- As explained in the section related to WFE verification, the thermal cartography derives from a thermal model that is verified/correlated during the satellite FM thermal vacuum test

The computed in-orbit geometry is then fed into grasp9 in order to perform the extrapolation taking account of the in-orbit geometry:

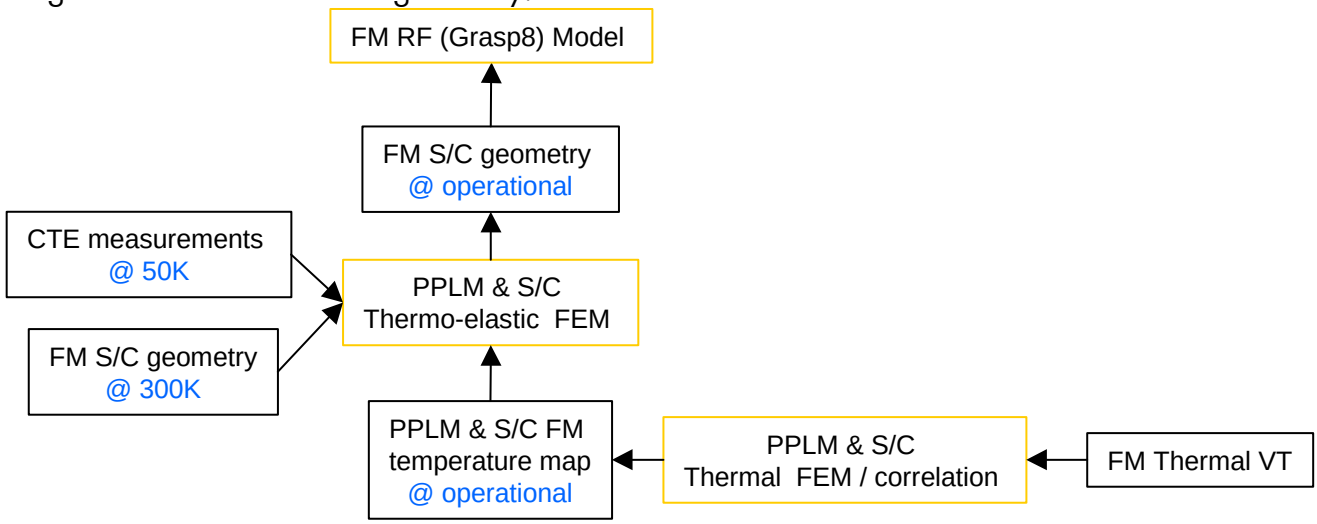

4.5 SPACECRAFT SELF EMISSION PERFORMANCE VERIFICATION

The approach proposed for the verification of the Spacecraft Self Emission performance follows the various steps of the corresponding analysis (See section 3). It can be split in three steps:

- a incident RF power verification
- a thermal verification
- a computation of the spacecraft self emission performance by combination of the two

Note: The issues linked with the PR illumination are not considered in the above verification logic: the energy levels at play here are not considered measurable.

4.5.1 Incident RF power verification

Based upon the current state of the art, the verification of the incident RF power (i.e. the incident power reaching the structural element from one detector) cannot be verified by test on Earth: the energy levels are too low to be measurable and the various contributors cannot easily be separated with such a complex specimen.

The corresponding verification therefore relies upon analysis.

Remark: The Planck Payload Architect study has anyhow shown that the spacecraft self emission was two orders of magnitude below the external straylight.

4.5.2 Thermal model verification

Due to the direct link between the fluctuations of the thermal laws and the spacecraft self emission performance, the thermal verification is part of the RF verification.

The thermal variation laws are classically verified using a thermal model correlated with a thermal test campaign. This classical verification addresses the temperature cartography and the time-dependent thermal variation laws of the spacecraft. It is achieved through the Thermal Vacuum Test performed on the Satellite Qualification Model (now split in two with a PPLM Cryogenic Qualification Model and a SVM STM) and the similar though reduced sequence performed on the Satellite FM.

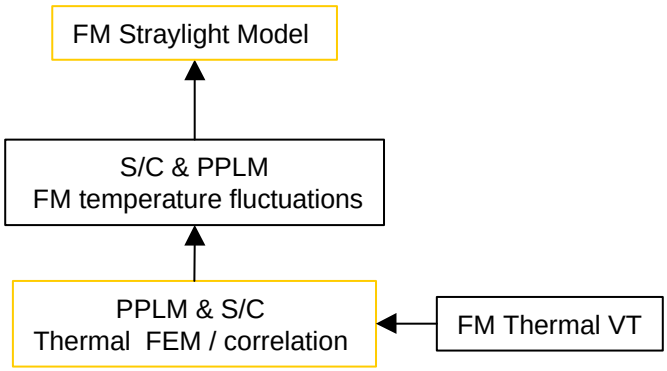

The outputs of the test are correlated temperatures & associated thermal law variations.

4.5.3 Flight performance computation

In final, the performance is verified by combining the results of the RF analysis (computation of RF incident powers) with the correlated thermal law variations in a similar way as used during the pure analysis phase:

Grasp9 model →	Computed RF incident Powers			→	Computed in-flight performance
Thermal tests → (QM + FM)	Correlated thermal model	→	Correlated thermal variation laws		

4.6 EMISSIVITY, APERTURE & FOV PERFORMANCE VERIFICATION

4.6.1 Emissivity

The emissivity is verified at reflector level. At system level, the contamination control (see H-P-1-ASPI-PL-0253) will monitor the contamination level on samples to ensure that the levels are the below the requirements.

4.6.2 Aperture

This design requirement is simply verified in 2 steps:

- dimensional verification at reflector level: this way the aperture size is verified
- inspection at system level: this way the absence of aperture obstruction is checked

4.6.3 FOV

This requirement basically sizes the baffle forbidden volume. This volume is derived from the optical interface drawing (PLAPLM0S4001A Ind A). Baffle dimensions are measured at ambient, and extrapolated to cryo to verify this requirement.

4.7 ADDRESSING THE VERIFICATION REQUIREMENTS

The verification requirements (See section 2) ask for measurements on a "representative RF model" ((AIMO-05), also called "elegant RF breadboard" (P-TEL-VER-052)) in order to establish the following parameters:

- Beam shape
- Straylight properties
- Polarisation properties

The above requirements are addressed as follows:

- The representative RF model is the RFQM.

- The beam shape issue is covered by the verification logic associated to the verification of the WFE and gain degradation (P-TEL-PER-030 & P-TEL-PER-035 performances).

- Straylight aspects are partially covered by the verification logic associated to the external straylight verification (spacecraft self emission cannot be directly assessed by test as explained above). This actually only covers the pattern area for which a rejection requirement is specified (i.e. a cone of 32° in the direction of the planets).

  The verification requirements therefore ask to complete the verification logic and to cover the whole space (4Pi steradians). This can be easily performed by extending the cuts proposed for the verification of the external straylight requirement, as depicted on the figure below:

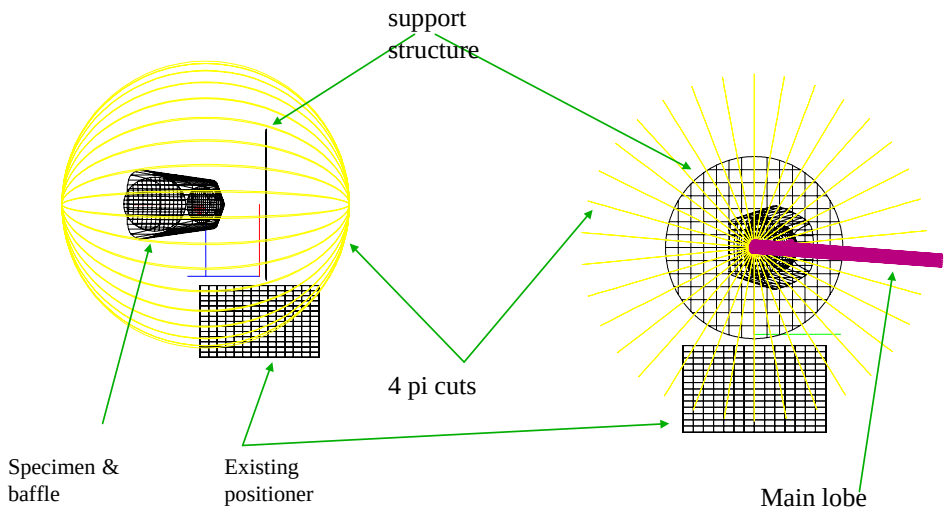

Figure 4.7-1 - Definition of the cuts proposed for the straylight-related measurements

In addition, a specific close look is proposed for the spill-over lobe that represents the most significant energy concentration outside the main lobe region.

The proposed meshing extends the approach selected for the verification of the external straylight requirement:

- Meshing in theta:
  - for the area where the Sun, Earth and Moon are located → intermediate meshing capability (angular steps of 0.5°) defined by the corresponding performance verification
  - for the spill over lobe past the primary → similar intermediate meshing capability (angular steps of 0.5°)
  - for the rest of the far out side lobe region → relaxed meshing capability (angular steps of 1°)
- Meshing in phi:
  - Identical approach for all cuts → angular steps of 5° to 10°

- In terms of measurement accuracy, the accuracy requirements derived from the gain degradation/ellipticity (main lobe region) and the external straylight (far out side lobes) performance verification are reconducted (as outlined in section 2, the verification requirements explicitly refer to the gain degradation/ellipticity performances for quantitative aspects).

- Concerning polarisation issues, not all horns are concerned: all LFI horns (at 30, 44 and 77 GHz) and only some HFI horns (100_1, 100_2, 100_3, 100_4, 143_1, 143_2, 143_3, 143_4, 217_5, 217_6, 217_7, 217_8, 353_3, 353_4, 353_5 and 353_6) present a dual polarisation. This is illustrated on the figure below.

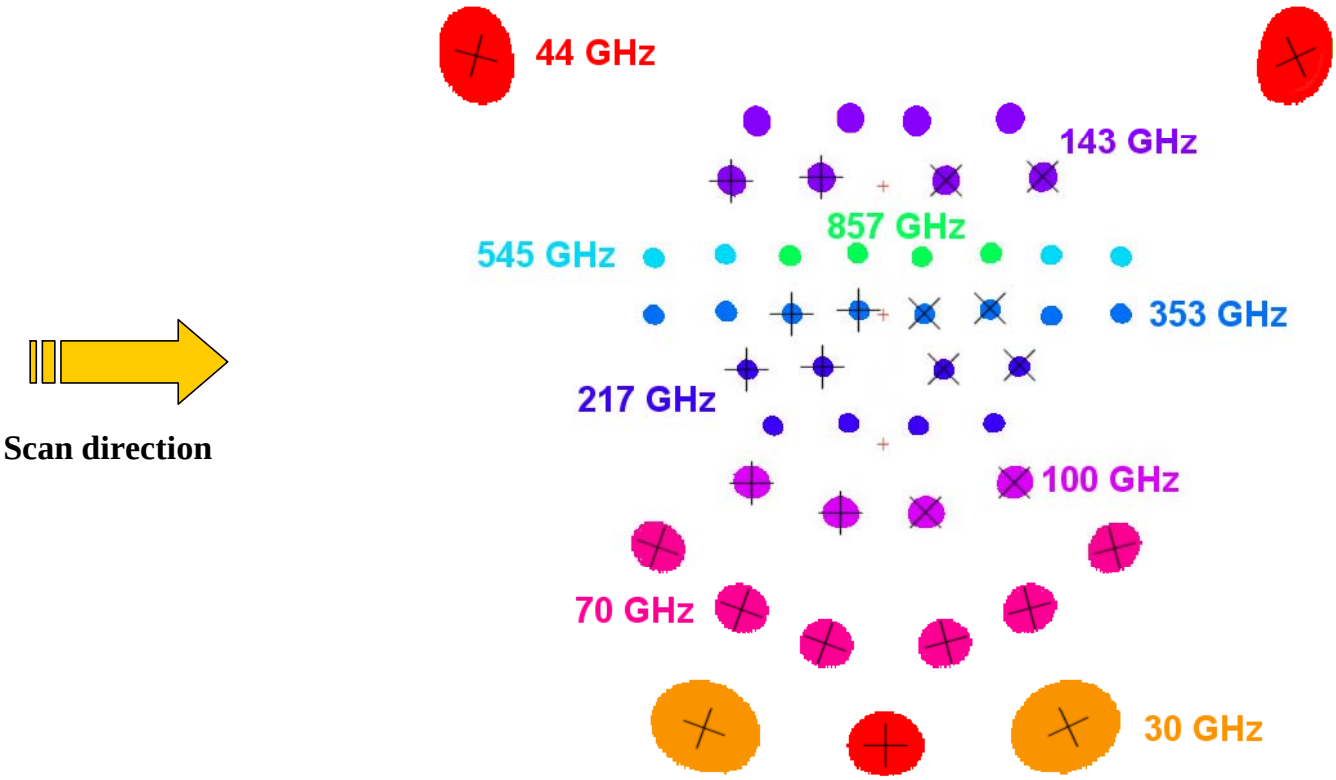

Figure 4.7-2 – Focal plane configuration (including polarisation)

(*Note*: The crosses indicate the direction of polarisation for the polarised horns)

Apart from the horns themselves, polarisation is due to the telescope. More precisely, the de-polarisation introduced by the telescope comes from its geometry (defining the angle of incidence of each ray on the reflectors for a given horn) and the properties of the reflector coatings.

Measuring the main lobe in Co- and Cross-polarisations (responses of Planck to a linearly polarised signal) allows to accurately correlate by test the geometrical (hence, the polarisation) model used for the RFQM and then to extrapolate it for the FM taking account of the differences between the FM and the RFQM (reflectors shapes, telescope & FPU alignment, horns characteristics) and between the RFQM test and FM in-flight configurations. The approach is indeed similar to the one already proposed for the main lobe measurements.

Such an approach however requires that 2 conditions are fulfilled:

- the test facility must not introduce significant perturbations in the polarisation pattern (this is not a problem with CATR's as their intrinsic quality wrt polarisation is around 10-5, hence negligible)
- The signals measured for Co- and Cross-polarisations indeed represent these quantities → this requires an alignment of the facility illuminator with the polarisation axis of the incident beam (that is classically achieved by a search for the max Co-polarisation signal via a rotation of the illuminator).

With the above 2 conditions fulfilled, only two responses perpendicular in terms of polarisation are needed to test the depolarisation introduced by the telescope.

Another solution could consist in implementing dual polarisation horns in the RFQM focal plane and to perform two series of Co- and Cross-polarisation measurements for each polarisation of the feed horn (hence, four measurements). This was however considered as somewhat superfluous and would anyway lead to more lengthy (and consequently more costly) tests.

The overall issue of how to address the verification requirements and incidentally of what measurements should be performed on the RFQM was presented at the Telescope Working Group and further addressed between ESA and the Instrument teams.

The number of polarisation planes needed for these measurements was largely debated. It came out that more than 2 planes of polarisation were needed. Options including either a minimum of 3 planes of polarisation or 2 planes of polarisation plus the associated phase needed to be measured.

An agreement was finally settled consisting in reducing the number of measured frequencies (2 frequencies among LFI frequencies: 30 & 70 GHz and 2 among HFI frequencies: 100 & 353 GHz will be measured) while improving the measurement of polarisation (4 planes of polarisation will be measured for all of the above frequencies so as to improve the knowledge of polarisation). Note that, by the end, measurement will be done at 320 GHz instead of 353 GHz for EGSE development constraints.

Similarly, the definition of cuts needed to cover the far out side lobes and the spill-over lobes was also settled through the same process.

The agreed detailed measurement plan is included in the RFQM ITT now issued (See RD6).

4.8 VERIFICATION LOGIC SUMMARY AND CONCLUSION

The following table summarises the verification approach detailed in previous sections for each requirement (performance verification or verification requirement). The verification objectives are addressed through the use of different models. The approach combines several types of tests (mainly RF, optical and thermal tests + inspections) associated to analysis (hence, models that are correlated by the tests):

Verification type	Requirement	Verification approach (Analysis / Test)	Comments
Performance Verification	Frequency plan	T + A	1 test for each frequency as a minimum on the RFQM (except for 857 GHz)
	Gain degradation	T + A	Model (including the theoretical performance) correlated by the RFQM tests and extrapolated for the FM
	Ellipticity	T + A	Idem
	External straylight	T + A	Idem
	Spacecraft self emission	T + A	Tests only address the verification of the thermal fluctuations
	WFE degradation	T + A	Anti-alignment prediction correlated by the QM cryo optical test + FM cryo optical test + budget approach for the other contributors
	Emissivity	T + A	Emissivity (reflection) verified by test at Reflector level + Contamination plan at Telescope & Satellite levels
	Aperture	T	Dimensional control at Reflector level + Inspection (no obstruction) at Satellite Level
	FOV	T + A	Baffle geometry control at ambient & extrapolation for operational conditions
Verification Requirements	Beam shape	T + A	Covered by gain degradation performance verification
	Straylight properties	T + A	Partially covered by external straylight performance verification (cuts extended to cover 4 Pi steradians with close look at the spill-over lobe)
	Polarisation properties	T + A	model (including the theoretical performance) correlated by the RFQM tests and extrapolated for the FM

Table 4.8-1 - Verification Logic (Synthesis)

Notes:

- Contamination is taken into account for the computation of the flight performance (i.e. in the analysis part of the verification logic). In terms of verification, it is however addressed separately (See the Cleanliness Control Plan). A contamination monitoring of the satellite is performed all along the manufacturing and integration phases.

- The above verification logic also takes into account the programme development constraints and in particular, the availability of Instruments and Reflectors equipment (QM & FM models). Indeed, all the tests performed on the RFQM could also be performed on the FM. This would however significantly delay the FM and add unwanted contamination to the reflector and instrument FM hardware.

As the optical & RF verification approaches are very similar, a tentative to combine the optical & RF verification approaches in common diagrams is presented in annex.

5. MODEL PHILOSOPHY

In order to encompass the complete scope of analysis, characterisations and tests linked with the verification of optical or RF performances and with the measurements specifically mentioned in the AIV requirements, the proposed Model Philosophy spans over the various levels of the Planck Product Tree.

The proposed approach first relies upon two dedicated Models specifically targeting the verification of RF performances:

- The Radio Frequency Development Model (RFDM)
- The Radio Frequency Qualification Model (RFQM)

Note: The possibility to include a specific RF sequence in the overall Flight Model (FM) test program was also addressed. The idea consisted in benefiting from the planned passage of the FM in the Alcatel CATR (for EMC-related measurements) so as to try and perform a limited RF test and complement on this model the verification logic. This however proved more difficult than one could initially think and is presently not retained mainly due to programmatic reasons (See section 5.3 below). The proposed verification approach is anyway complete without this additional test.

Similarly to the above RF models, the Planck QM & FM Telescope models provide the cornerstone for the verification of the optical performances. This is addressed via dedicated sequences (Optical cryogenic tests) implemented in the overall AIT sequence for each of these models.

In addition and as evidenced by the discussion about the verification logic, the following items also form an integral part of the Optical & RF verification approach:

- Materials & components (thermal & thermo-optical properties characterisation)
- Planck Reflectors QM & FM models (optical cryogenic tests, …)
- Planck FPU QM & FM models (horn relative alignment, horn characterisation, …)
- Planck Satellite QM & FM models (thermal test sequences, …)

The main building blocks of the Optical & RF verification approach listed above are detailed in the following paragraphs. The test objectives, test frequencies, specimen, associated numerical model (if any) and facility requirements are provided for the main RF & Optical models and test sequences directly under Alcatel responsibility.

5.1 RADIO FREQUENCY DEVELOPMENT MODEL (RFDM)

5.1.1 RFDM test objectives

Early in the programme, during phase B, a cross validation between the numerical and the physical models will be achieved through a dedicated model (the RFDM) & the associated test campaign.

The first test objective of the RFDM is to validate the modelling method (Grasp9) and the associated numerical model (combination of multi-gtd and PO with identified straylight paths and levels) as early as possible in the phase B.

The second test objective of the RFDM is to validate the feasibility of measurements with a huge RF dynamic (around 100 dB required) at the Planck frequencies (at least at some of them).

5.1.2 RFDM Test Frequencies

The proposed test frequencies are 30 and 100 GHz:

- 30 GHz has been selected because it is the lowest frequency. Compared to other frequencies, 30 GHz is the worst frequency from a diffraction point of view.

- 100 GHz has been selected for being still quite low in frequency though far from 30 GHz. At this frequency a new set up measurement has to be used (spectrum analyser technique). In addition, 100 GHz is well inside the guaranteed operating frequency range of the Compact Antenna Test Ranges. (*Note*: When originally defined, this was also a common frequency for both LFI & HFI. This is not true anymore.)

5.1.3 RFDM specimen

The RFDM specimen is architectured around the existing Archeops set of Reflectors. Two configurations will be tested: with & without the baffle in order to assess in particular the effect of the baffle wrt the spill over and some far out side lobe directions (where the baffle is predicted as having a noticeable effect).

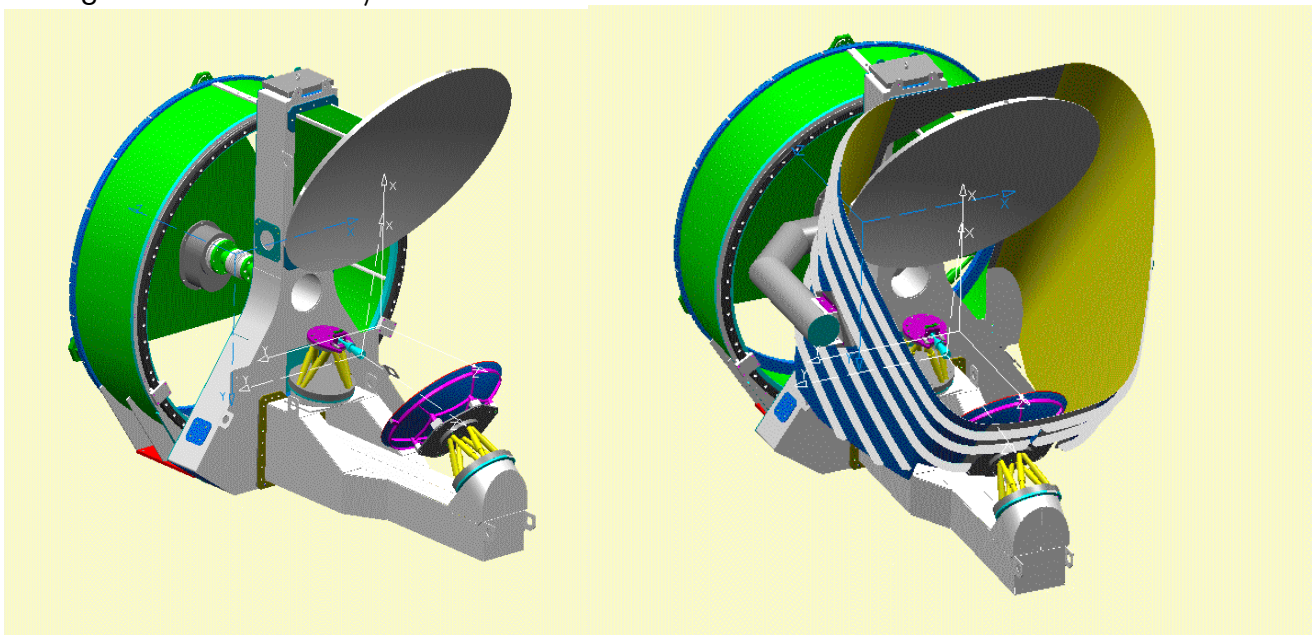

Figure 5.1-1 - RFDM Specimen (Configurations without & with baffle)

The Archeops telescope has been manufactured to be used at the HFI frequencies (143 GHz and higher). The surface accuracy is perfectly suited for and representative of the Planck one. The Archeops geometry is a dual gregorian reflector configuration. The general diagram behaviour is the same as the actual Planck one. In other word, the main beam is close to the telescope line of sight with a spill over lobe passing the primary. The surrounding structure (baffle) deeply shadows the diagram in the rear telescope direction: most of the energy is rejected in the forward telescope direction. This diagram is then similar to the Planck one.

The Archeops reflectors are made of metal and manufactured for RF operation up to 353 GHz. The surface manufacturing can then be considered as excellent at 100 GHz and lower frequencies. The electrical behaviour of the reflectors can also be considered as ideal thanks to the metal electrical properties. The reflectors are fully made of metal and not only metallized on the active RF surface. That is why comparatively the electrical behaviour of the RFDM is considered as better than any other hybrid model.

5.1.4 RFDM RF Model

The Archeops telescope is made of aluminium that can be considered as perfectly conducting and hence reflecting. The associated numerical model has the default surface property set to infinitely conductive. This is of great interest for the cross validation between the numerical and the physical models.

The Archeops telescope will be accurately mechanically measured and optically aligned before RF testing, the obtained metrology data (not the ideal surfaces) being introduced into the RF model. Then, the results will be compared with the RF test measurement data keeping in mind that the uncertainty introduced by the measurement (facility, calibration, etc) shall be much lower than the expected model/metrology discrepancies.

The RFDM baffle is also made of thick aluminium and is consistent with the Planck baffle geometry. (*Note*: This was true at the time of the RFDM tests → since then, an extension has been introduced at the front side of the baffle to further reduce the illumination of the PR by the moon).

To summarise, the Archeops telescope is precisely manufactured wrt the test frequencies and fully metallic. Hence it can be considered as very close to the numerical model hypothesis (ideally manufactured and infinitely conductive).

5.1.5 Test facility requirements for the RFDM

The selected test facility is a Compact Antenna Test Range.

The CATR will be equipped with a RF chain set up operating at 30 GHz and 100 GHz and reaching a measurement dynamic of 90 dB at these frequencies (100 dB as goal).

The tests will be performed over all space directions in order to produce measurements of the main lobe, of the spill-over lobe and of the far out side lobes (actually, some cuts). The CATR has

to be equipped with a positioner of high precision (at least 0.005°) allowing the pointing over 4pi steradians (for far out side lobe measurement).

This positioner shall also be able to point the main beam of the device under test into a pre-defined acquisition grid. This acquisition grid will be defined versus frequency (the width of this grid decreases when the frequency increases).

The CATR shall deliver measured patterns in a TICRA compatible file format for the main lobe and the far out side lobe cuts.

As a conclusion, the RFDM is a simple and reliable model at 30 and 100 GHz. The RFDM tests will then be used to validate the work performed by the TICRA Company on the numerical model. The RF tests at 30 and 100 GHz allow in addition to cover most of the critical points associated with RF measurements at such frequencies. The lessons learnt from this test campaign will be valuable either to perform the future Planck RF tests on the qualification model.

5.2 RADIO FREQUENCY QUALIFICATION MODEL (RFQM)

5.2.1 RFQM Test objectives

The RFQM first test objective is to verify the flight performances at all measurable frequencies (at least to provide the main block verification for these performances):

- The first test objective is to measure the main lobes (with polarisation information) at least at the frequencies that can be practically measured (i.e. up to and including 353 GHz). Test at higher frequencies (i.e. 545 GHz but not 857 GHz that is considered too critical) will be asked in the RFP for the RFQM test: test capabilities (and eventual limitations) at these frequencies will have to be addressed in the answers to the corresponding ITT. The bidder will have to demonstrate its ability at these frequencies.

- The second test objective is to measure the far out side lobes (including the spill-over lobe) relatively to a level defined by the scientists. The other scientists' requirement is to obtain the side lobes with a known accuracy when the level is over the noise limit (in other words when the side lobe levels are within the dynamic range of the measurement).

This test will take into account all second order phenomena that cannot be modelled (micro-cracks, reflector contamination, actual reflector edges). Each of these contributors will be analysed and used in the telescope performance budget.

5.2.2 RFQM Test Frequencies

The tests will be performed at 30, 70, 100 and 320 GHz as a minimum. Capabilities to perform tests (with eventual limitations) at 545 GHz will also have to be addressed (this series of tests being subject to an ITT, this has been requested in the related ITT requirements – See RD6).

Note: There was a common agreement at the Telescope Working Group that tests at 857 GHz were not practically feasible within reasonable technical, programmatics & cost constraints.

5.2.3 RFQM specimen

The RFQM will be built around the QM hardware and includes:

- The QM reflectors
- a partial sub-set of the QM PPLM hardware (telescope, baffle, groove n°3, MLI skirt closing the cavity between groove n° 3 & the baffle & Cryo-Structure struts to support it all)
- dedicated flight representative horns at the selected frequencies

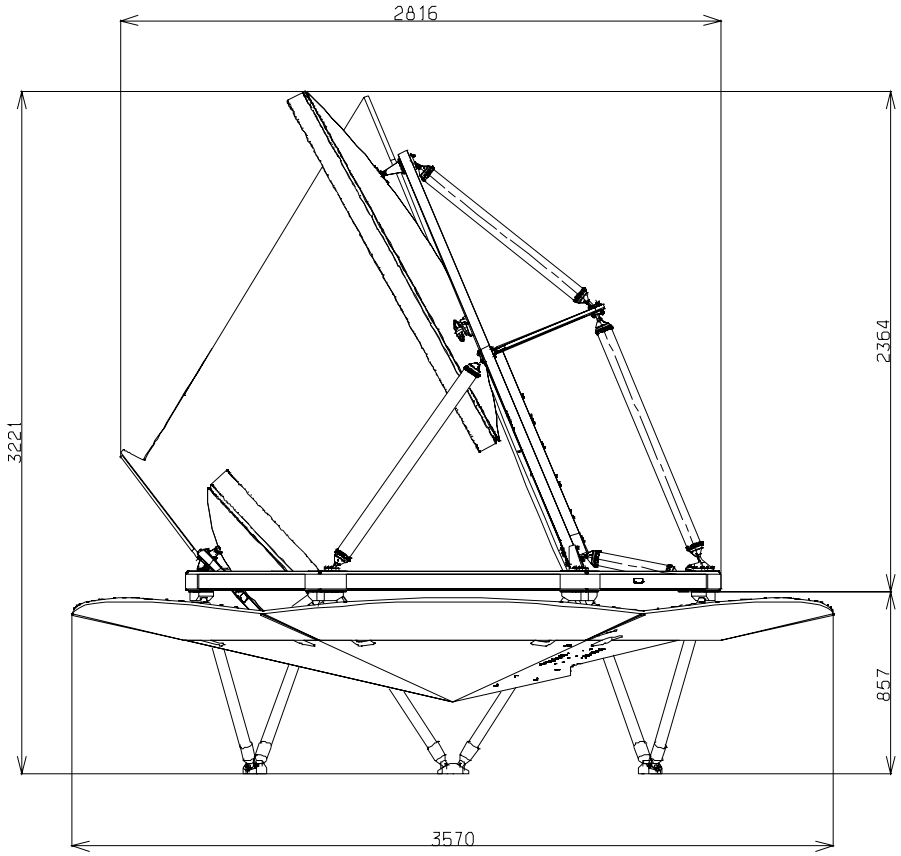

Figure 5.2-1 - RFQM Specimen (test horns not depicted)

Thanks to its building hardware, the RFQM is then very close to the flight design on the following points:

- reflector edges

- reflector surface quality including thickness of coating, micro-cracks and roughness
- telescope image quality.

The above points would not be seen on a telescope mock up, its representativity would be always questionable and would open long discussions with the scientists about the validity of the results.

5.2.4 RFQM RF Model

This RF model will be derived from the model established by TICRA as part of the RF Expertise study. With regards to the original TICRA model, the following data will be added/updated:

- QM Reflectors characterisations (i.e. shape at ambient temperature)
- QM test horn characterisation (horn pattern, phase centre position)
- Telescope alignment data (derived from alignment measurements)
- FPU alignment data (as issued of the RFQM FPU alignment process)

As for the RF model itself, the RF modelling will follow the rules edited by TICRA during the RF Expertise study. In particular, the modelling principle (multi-gtd with local PO patches) and the various straylight paths identified during this study will be reproduced.

After correlation on the RFQM, the RF model will be reproduced with an identical structure for the FM and consequently for the prediction of the in-flight performances. As explained in the above section related to RF verification, the only modifications between the RFQM and the FM RF models will be the input data (Reflector shape, horn data & Telescope + FPU alignment data).

5.2.5 Test facility requirements for the RFQM

The preferred test facility is a Compact Antenna Test Range, particularly for the lower frequencies (this will also allow simpler comparison with the RFDM). Other types of facility are however to be considered for higher wavelengths (e.g. based upon a holographic techniques such as developed by Millilab). The corresponding main requirements for this (these) facility(ies) are given below:

- The facility has to be equipped with a RF chain set up operating at all selected frequencies. Also and as the targeted frequency range is not classical, the behaviour of the facility absorbers (anechoids) has to be known at these frequencies.

- The RF chain shall reach a measurement dynamic of 90 dB (100 dB as goal). This dynamic requirement can eventually be adjusted frequency per frequency.

- The tests have to be performed over directions spreading over 4pi steradians (measurement of the main lobes, of the spill-over lobes and of cuts distributed in the far out side lobe region). The facility has to be equipped with a positioner of high precision (at least 0.005°). For the measurement of each main lobe, this positioner shall be able to point the main beam of the tested specimen into a pre-defined acquisition grid. This acquisition grid shall be defined versus frequency (the width of this grid decreases when the frequency increases).

- The facility shall deliver measured patterns in a TICRA compatible file format.

5.3 FLIGHT MODEL (RF TEST SEQUENCE)

As mentioned in the presentation of the overall model philosophy, the idea of introducing a RF Test sequence in the overall FM sequence was discussed tough it proved difficult to implement in the end.

The principle of such a test would consist in operating the satellite inside a CATR (it is planned that the FM satellite will be tested inside the Alcatel CATR for the EMC sequence). At least one horn would then be operated so as to reproduce some of the RFQM measurements even in a limited manner (e.g. main lobe measurements).

Considering the existing LFI & HFI horns, it was evidenced that even the LFI 30 GHz channels would have too limited performances in terms of sensitivity at ambient (nominally all LFI & HFI channels are planned to be operated in cryogenic environment). The idea then converged to a dedicated test horn that would have been associated to electronics capable of operating at ambient. This implied the possibility of dismounting totally or partially (the test horn would then have to fly after being disconnected from its test electronics).

The above issue was addressed jointly with ESA and the Instrument teams through the Telescope Working Group. Two main implementation options were studied:
- A test horn located on the external side of the FPU main frame
- A test horn located inside the FPU

The first option (external accommodation) was quite simple in terms of accommodation & dismountability. Unfortunately, the image quality at such an ex-centred location was too degraded to provide any sensitivity wrt alignment at all.

The second option (internal accommodation) has been selected. A 320 GHz dismountable horn has been implemented in the flight FPU and test in double path configuration is planned on the FM S/C. Preliminary test with such configuration has been performed in the frame of the RFQM test campaign. No show stopper has been identified but final feasibility assessment is in progress.

The issues linked with such a test are presented below (in a similar way as for the other tests, tough using the conditional form).

Note that other solutions were also considered. These include a test horn fixed outside the FPU main frame but positioned in front of the FPU (and removed after the FM test). Other types of facilities were also evoked but this would have meant moving the FM satellite to another site and back with all the constraints that such a transport implies (delays, containers, cleanliness, risks).

5.3.1 FM RF Test Objectives

The Flight Model RF test objectives would consist in providing an additional verification of the flight performance through an end to end test. Practically, the test will would consist in measuring

the main lobe for a reference test horn and in comparing the results with those obtained on the similar horn implemented on the RFQM.

5.3.2 FM RF Test Frequencies

The test frequency would be 320 GHz. This frequency was retained so as to provide the best sensitivity in terms of alignment (focus). The reference test horn is provided by HFI.

5.3.3 FM RF Test Configuration

The Flight Model (i.e. the Planck spacecraft) would have to be accommodated on the positioner of a Compact Antenna Test Range similarly to what is planned for the RFDM and for the RFQM.

5.3.4 FM RF Model

As explained in the section presenting the RFQM, the RFQM RF model will be reproduced with an identical structure for the FM and consequently for the prediction of the in-flight performances. This will be undertaken after correlation of the RFQM RF model by the RFQM tests. The only modifications between the RFQM and the FM RF models will be the input data (Reflector shape, horn data & Telescope + FPU alignment data).

5.3.5 Test facility requirements for the FM RF Test

The CATR has to be a class 100 000 clean room (the specimen is the actual Planck FM satellite and must comply with the associated cleanliness plan). This should not be a problem for the existing facilities. (*Note*: Cleanliness aspects are dealt with at system level taking account of the whole AIT sequence).

The CATR will be operate in a double pass configuration. The Tx horn placed in the feed room will be replaced by a quasi optical illuminator (QOI) made of a TX module, Rx module and and beam splitter. The QOI is provided by ESA.

In addition to the similar positioning requirements already expressed for the RFDM and the RFQM, the CATR would have to accommodate the Planck satellite Flight Model on its positioner.

5.4 PLANCK TELESCOPE QM CRYOGENIC TEST (VIDEOGRAMMETRY)

5.4.1 Test Objectives

The objectives of the Telescope QM Cryogenic test are:

- The correlation of the thermo-elastic model
- The prediction of the FM anti-alignment and of the associated prediction inaccuracy (hence the estimation of the WFE)

In practice, the test consists in cooling down the Telescope structure from ambient down to cryogenic temperature and to follow the structure behaviour (i.e. the relative position of various points of the structure between ambient and cryogenic conditions).

Originally a configuration and a principle similar to the ones planned for the Telescope FM cryogenic test (i.e. a cryogenic-optical test using the same OGSE) was planned for this test. Due to the unavailability of QM Reflectors on time, optical measurement methods had to be discarded. A trade-off study led to the selection of a videogrammetric measurement principle. Such a technique allows to provide the position of a series of points materialised by targets with a typical accuracy in the range of 20 to 30 μm (this is actually dependent on the target observation conditions).

5.4.2 Test Specimen & Configuration

The test specimen is constituted of the bare Telescope structure (without Reflectors) equipped with videogrammetric targets. These targets are mounted either directly on the Telescope structure or on stable supporting structures (i.e. made of Invar). This second approach is preferred for the key interfaces (Reflectors, FPU) so as to allow for the implementation of redundancies (and thus so as to increase the accuracy).

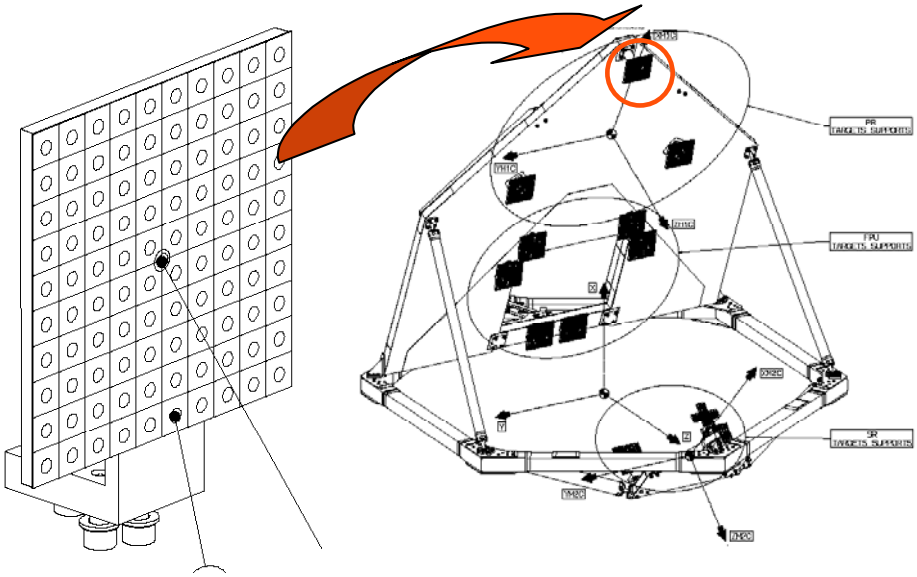

Figure 5.4-1 – Telescope QM Cryogenic Test Specimen

The Telescope has in turn to be supported by a stable and known GSE capable of withstanding the variation in thermal conditions between both measured configurations (ambient and cryogenic). Again, a trade-off study showed that a stable Invar structure (called Thermal test Adaptar or TTA) with simple thermal control was needed for this purpose. This structure has to interface with the Telescope via struts representative of the Cryo-Structure struts (the idea is again to introduce displacements that are controlled and similar to those predicted for the flight environment).

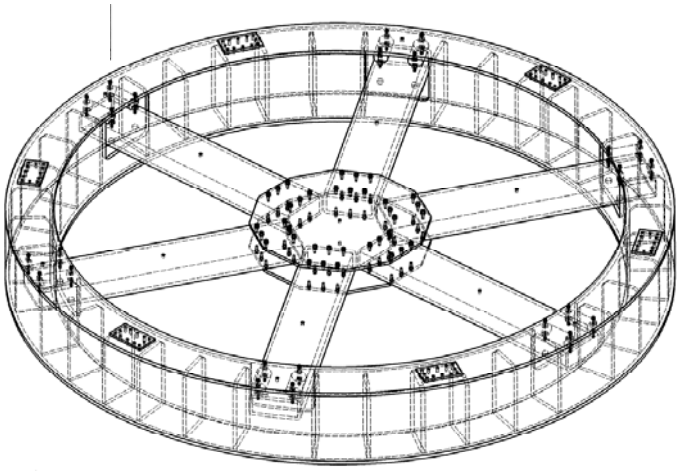

Figure 5.4-2 - Telescope QM Cryogenic Test GSE (TTA)

The videogrammetry camera has to be rotated so as to increase the number of angular positions under which each target (or group of targets) is seen. A trade-off study showed that the Baffle had to be removed as it limited this accuracy by blocking possible observation angles. The overall configuration (Specimen + GSE + Videogrammetric equipment) is depicted on the figure below:

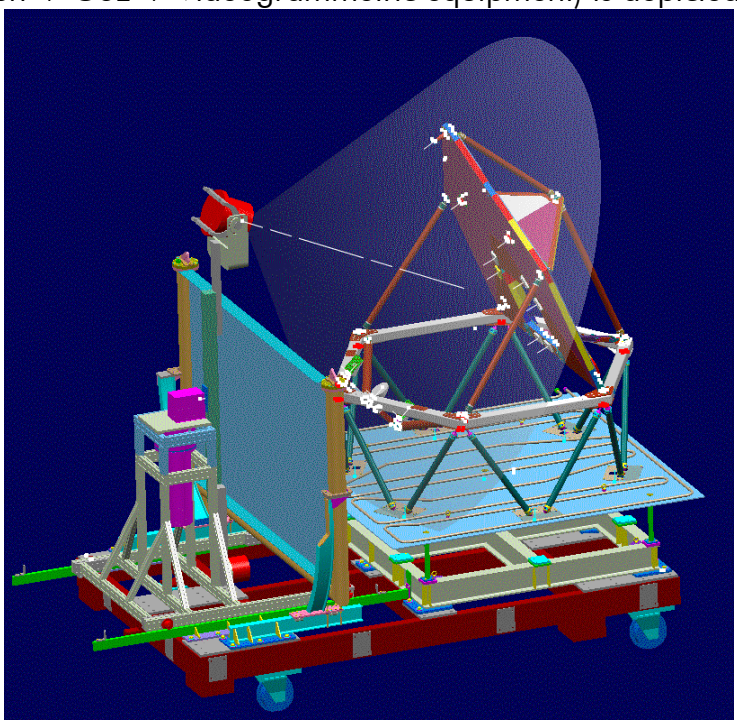

Figure 5.4-3 - Telescope QM Cryogenic Test Configuration

5.4.3 Test Facility

The required test facility is a cryogenic vacuum chamber. The initial idea consisted in using the same facility as for the Telescope FM Cryogenic test (i.e. the FOCAL 5 facility of CSL). Due to programmatic constraints, this was not possible. An alternative solution was found consisting in testing the specimen in Alcatel Cannes facility. The consequence was a limitation in the

achievable temperature (between 90 K & 100 K instead of around 40 K at CSL) due to the absence of Ghe equipment in this facility (the facility is only equipped with LN2 shrouds).

The figure below depicts the test configuration inside this facility.

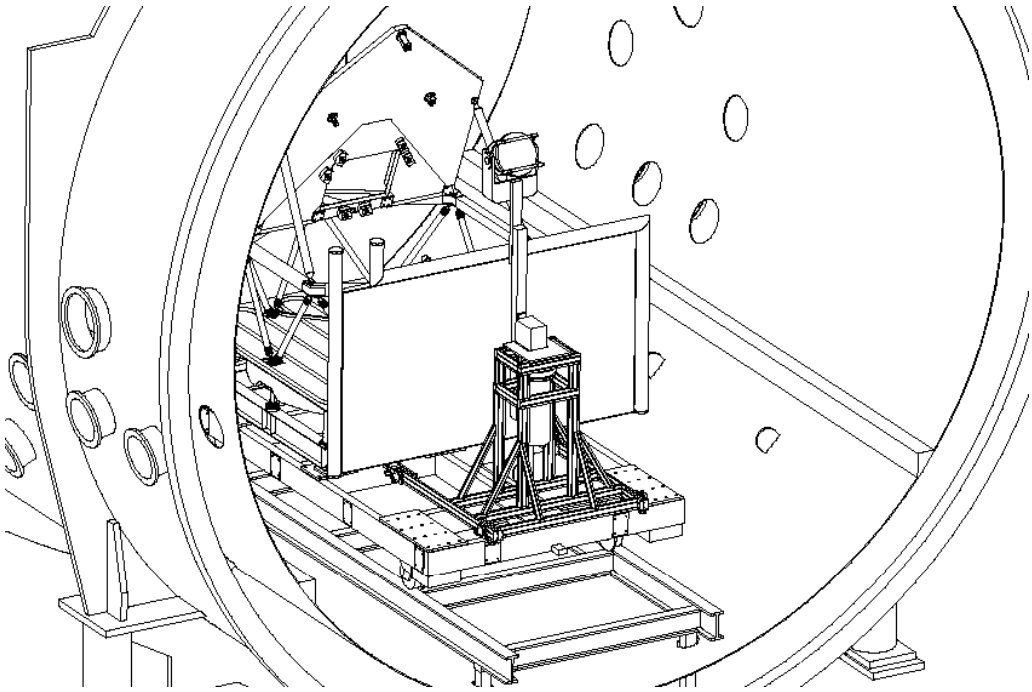

Figure 5.4-4 - Telescope QM Cryogenic Test Facility (Alcatel Cannes)

5.5 PLANCK TELESCOPE FM CRYOGENIC OPTICAL TEST

5.5.1 Test Objectives

The main objective of the Telescope FM Cryogenic Optical test is to measure alignment of the telescope including the FM reflectors and the FPU structure (LFI main frame) in order to compute the Telescope WFE. The in-flight WFE in then derived through a performance prediction model architecture around the Code 5 software.

The detailed objectives of the test is to measure :

- The relative position and orientation between the PR BFE axis (OM1) and the SR BFE (OM2) at 100K
- The evolution of the position and orientation of the PR BFE axis (OM1) wrt the FPU interfaces between ambient temperature and 100K
- The evolution of the position and orientation of the SR BFE axis (OM2) wrt the FPU interfaces between ambient temperature and 100K
- The evolution of the position and orientation of the FPU interfaces wrt the PPLM-S/C interface between ambient temperature and 100K.

5.5.2 Test specimen and configuration

The test configuration is described in the following figure. It is made of :
- the cone n°4 of the SVM
- the QM cryo struts
- the FM telescope (FM structure and FM reflector) with LFI QM main frame

Targets are bonded on the reflector and the telescope structure. Two fixed camera are implemented in the vacuum chamber and the test specimen is rotating from –180° to +180°. Images are recorded every 1.25 °

Test is performed in the ESTEC LSS vacuum chamber.

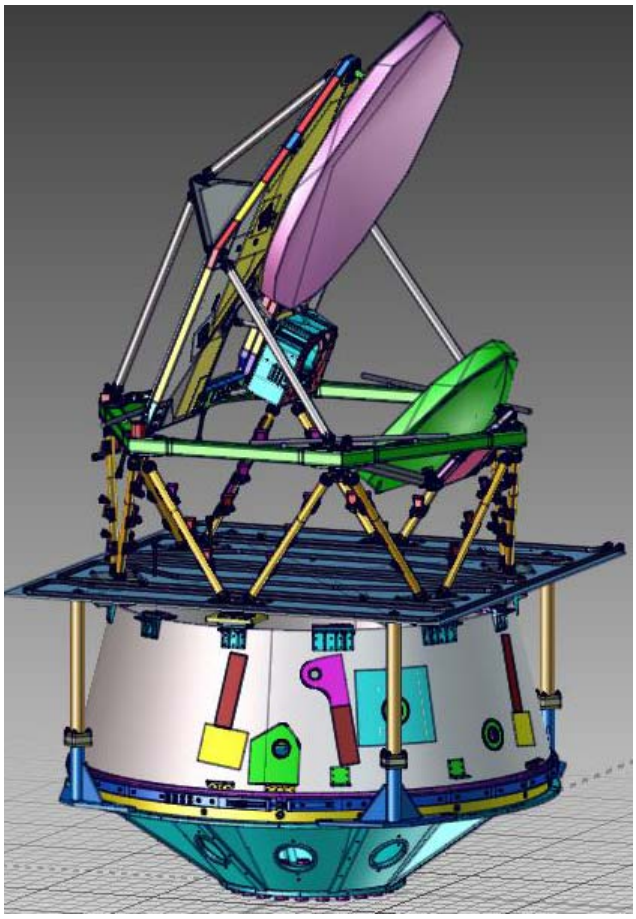

5.5.3 QM Reflectors

QM Reflectors are used for the RFQM model and must be characterised accordingly. As explained in the previous section dealing with the verification of optical & RF performances, the following characterisations are needed:

- WFE & Best Fit Ellipsoid (BFE) characterisation
- Sensitivity to I/F laods

These characterisations are needed at ambient. In addition, similar WFE & BFE characterisation under cryogenic conditions are also required so as to measure the cool-down behaviour (WFE, position/displacement of the BFE). In particular, the dimpling effect that appears at cryogenic temperature has to be characterised prior to the FM tests as the dimpling behaviour impacts the measurement principle retained for the FM Telescope Cryogenic Optical test.

This set of information allows to align the RFQM and to predict the RFQM WFE & RF performances (for correlation with the RF tests).

5.5.4 FM Reflectors

A similar characterisation (at ambient & under cryogenic environment) is required for the FM Reflectors. This time, the data is used for the alignment of the FM (actually for the anti-alignment) and for the prediction of the in-flight performances.

5.6 PLANCK FPU TESTS

5.6.1 QM FPU

Similarly to the Reflectors, the FPU must be characterised. This includes the following:

- Horn characterisation: Pattern & position of the centre of phase
- Internal FPU alignment: LFI vs HFI & horn-to-horn
- Global FPU alignment : LFI-HFI vs mechanical interfaces

For both types of characterisations, effects of cryogenic environment have to be characterised so as to take account of cool-down effects: geometrical effects (alignment + horn dimensions) + horn frequency & pattern modifications. The position of the FPU focal surface wrt the mechanical interfaces at operational temperature shall be provided by instrument for alignment purpose at telescope level

5.6.2 FM FPU

A similar characterisation (at ambient & under cryogenic environment) is required for the FM FPU.

5.7 THERMAL & THERMO-OPTICAL CHARACTERISATIONS & TESTS

5.7.1 Material & Component Characterisations

3 different sets of tests performed at material level act for the WFE and Gain performance verification :

- CTE measurement over the full temperature range
- E modulus measurement at operational temperature

The characterisation of these parameter is necessary to correlate properly the thermoelastic model which is uses to to extrapolate the QM cryo performance from 100K to 40 K and define the anti alignment of the FM.

- CTE evolution versus thermal cycling

The characterisation of this one is necessary to guarantee that the FM alignment verified at 40k during the FM cryo test is still valid after the telescope cool down of the FM S/C cryo test and the in orbit cool down.

The stiffness measurement of the blades which support the grove onto the cryo-struts (test performed at component level) act also for the WFE and Gain performance verification. Indeed, no WFE measurement at cryo temperature is performed at PPLM level (i.e. including the groove). The measurement of the blade stiffness will allow to introduced correlated interface loads induced by grooves thermo-elastic effects.

5.7.2 Satellite CQM Thermal Test

The telescope FM cryo test configuration will not provide an thermal environment inducing telescope thermal map (gradient) representative of the in flight configuration. Indeed, this thermal map is driven by the instrument heat loads which are included in the telescope FM cryo test. On the other hand, the S/C CQM test will allow to measure the thermal temperature maps induced by HFI instrument CQM heat loads and LFI heat load allocations. These thermal maps will be used to compute the telescope deformation at operational temperature and the corresponding WFE and gain performances.

The CQM test will be also used to correlate the transient thermal behaviour of the PPLM wrt temperature fluctuations at instrument interfaces. This will be done by injecting a thermal power with heaters and analysing the temperature response versus time of optical cavity elements. The correlated model will be used to compute the temperature fluctuation of the critical elements and then, the spacecraft self emission performance.

5.7.3 Satellite FM Thermal Test

The FM cryo test will provide temperature map induced by the FM instrument heat loads. It will be used to compute the in flight telescope deformation and finally the in flight WFE and gain performances.

ANNEX 1: SYNTHETIC VERIFICATION LOGIC

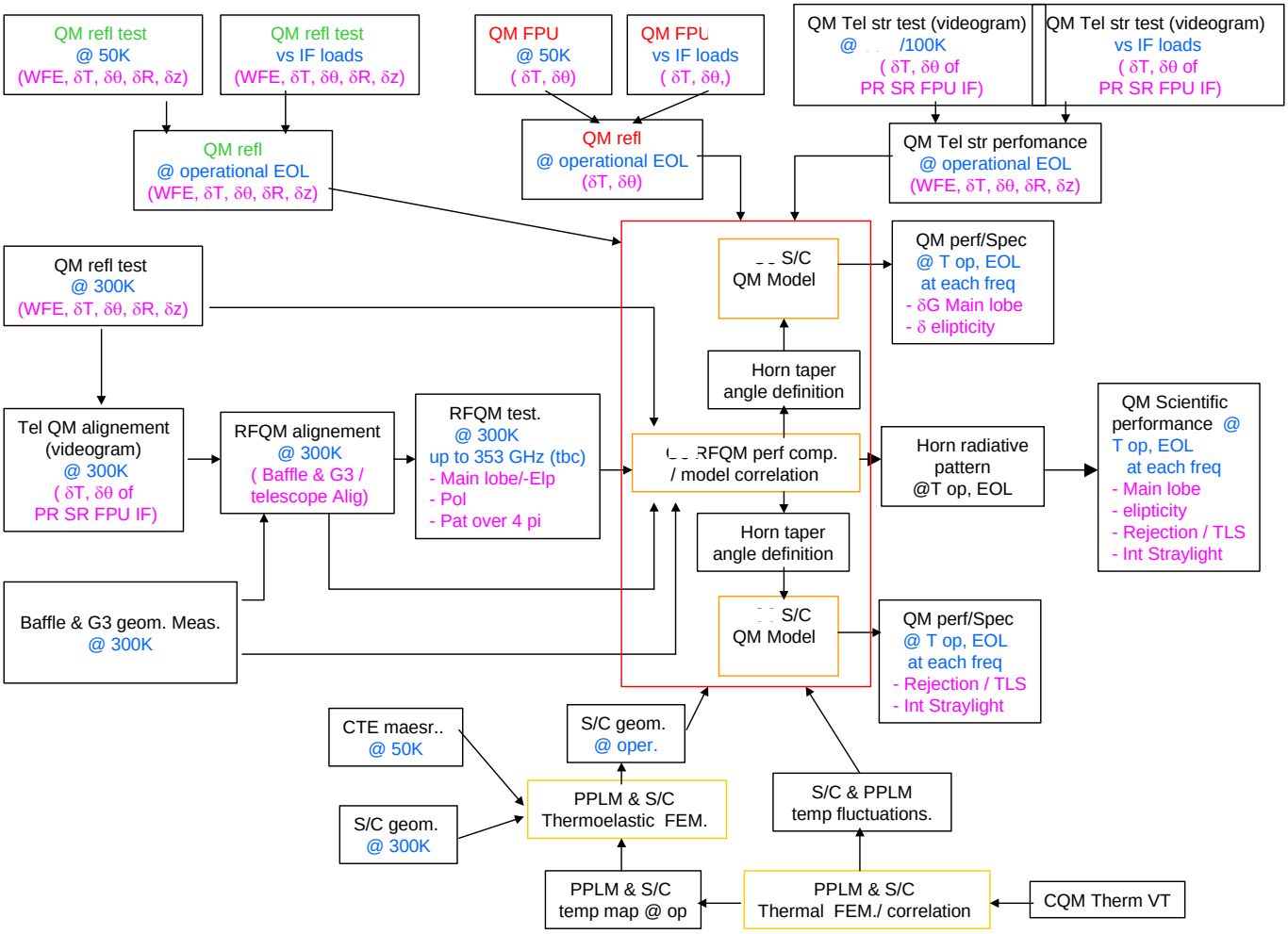

Figure A1-1 - QM Optical & RF Verification Logic

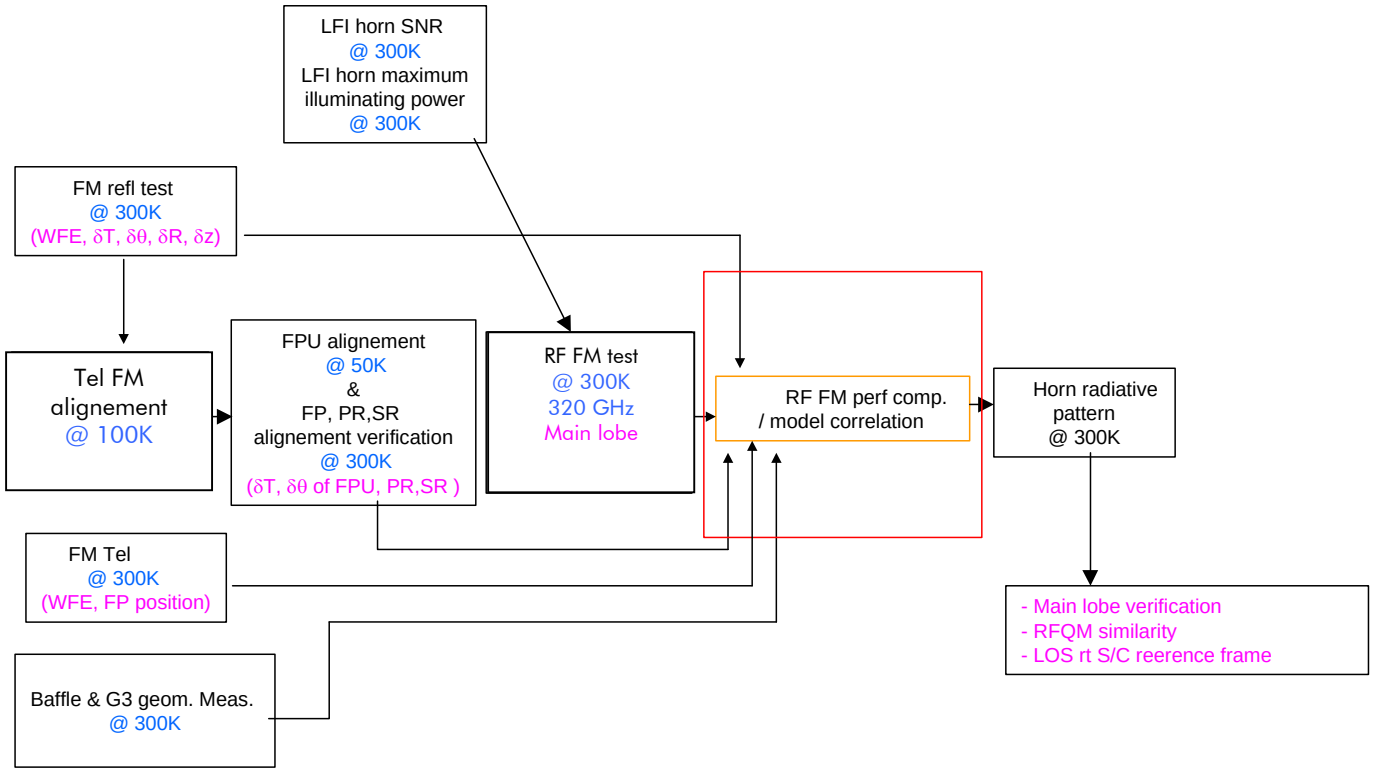

Figure A1-2 - FM Optical & RF Verification Logic (1/2)

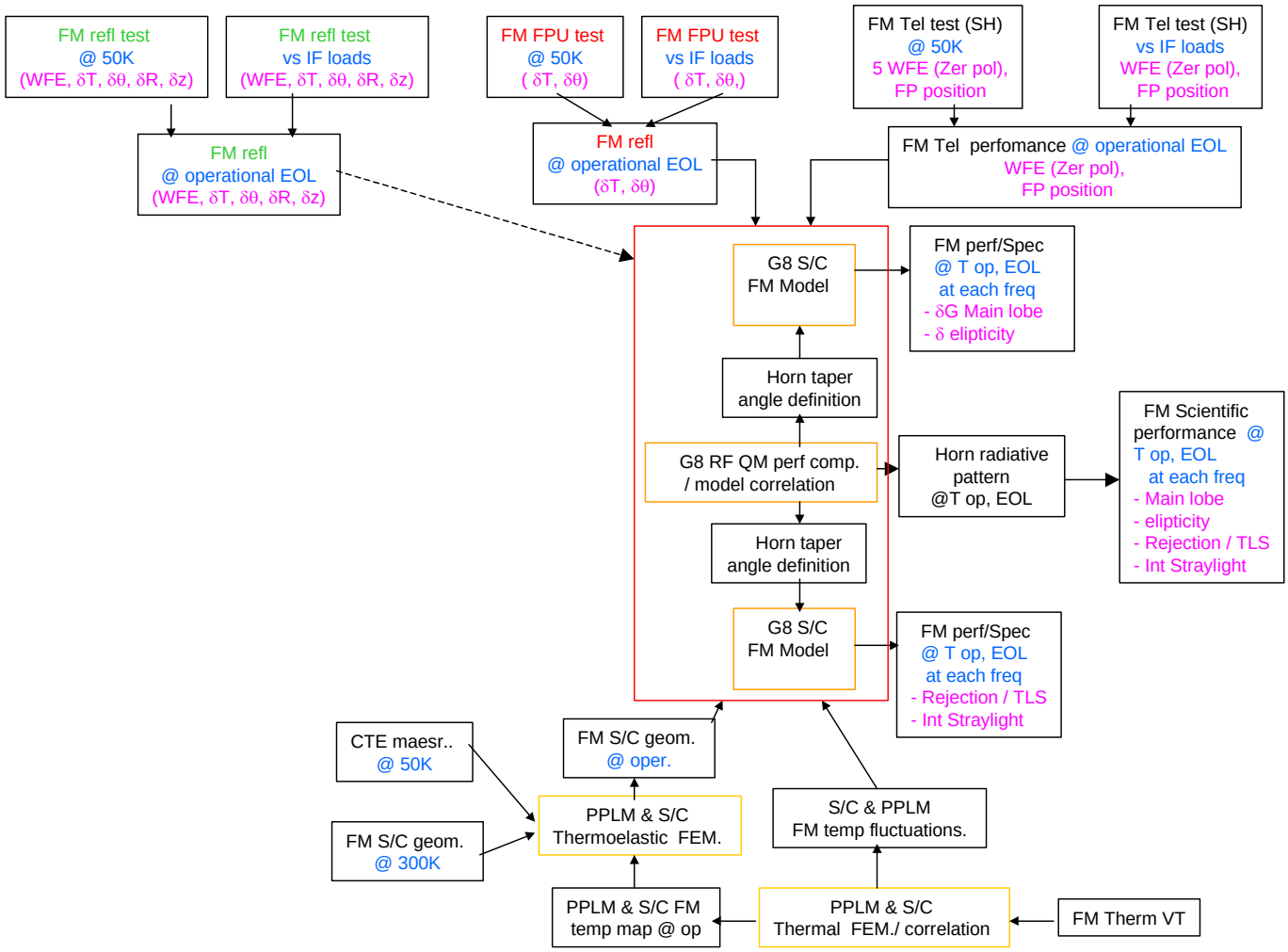

Figure A1-3 - FM Optical & RF Verification Logic (2/2)

Detailed verification logic per model for each specified performance

WFE (QM, FM)

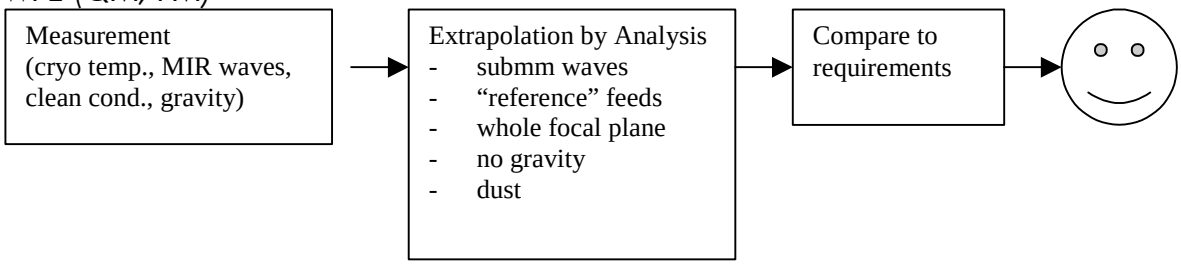

RF main beam properties

- Peak gain degradation, ellipticity (QM only)

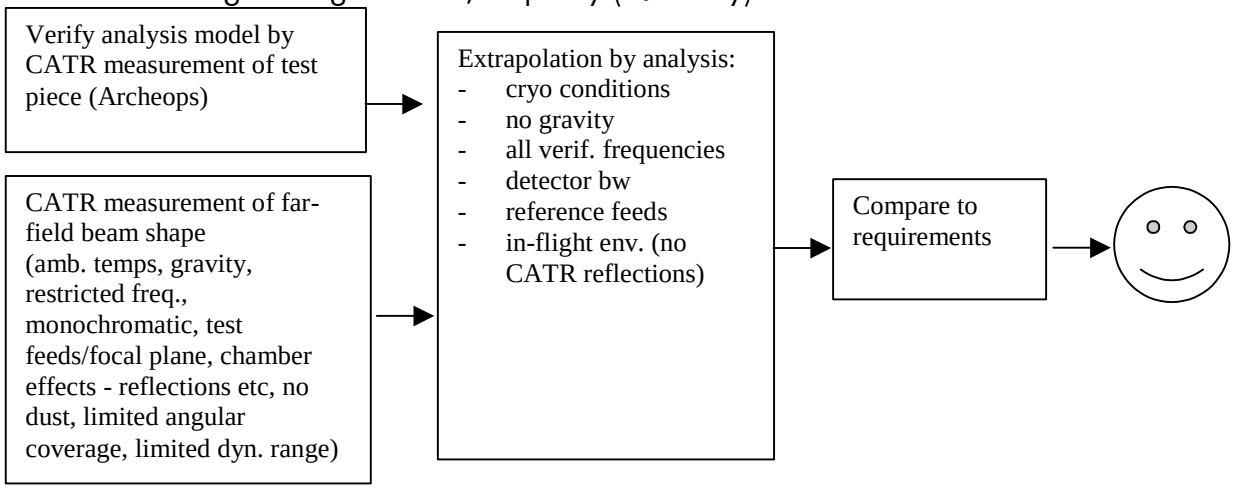

- Peak gain degradation, ellipticity (FM only)

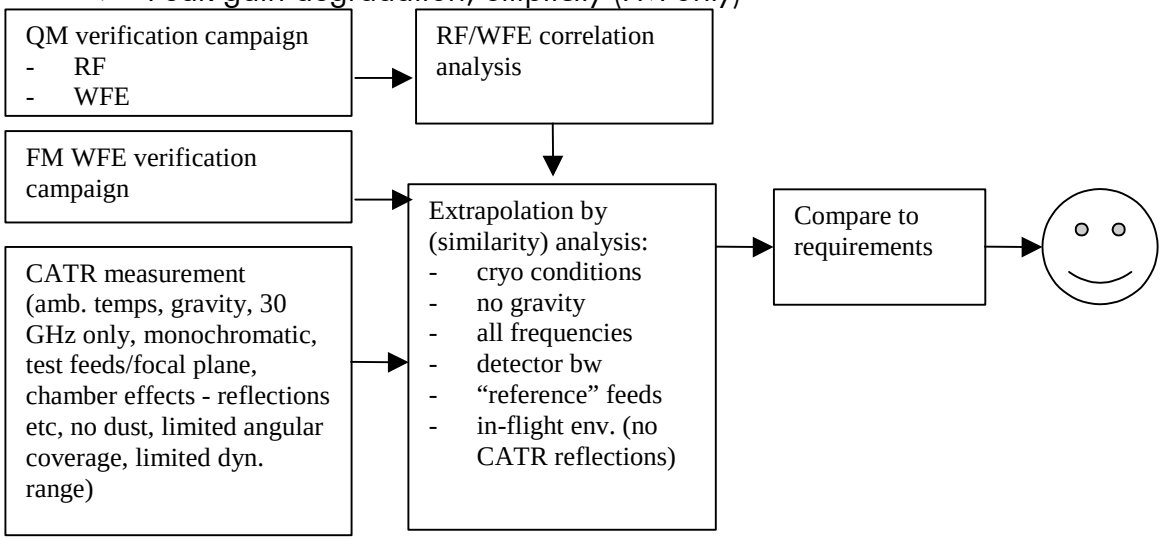

- Shape, polarisation (FM only)

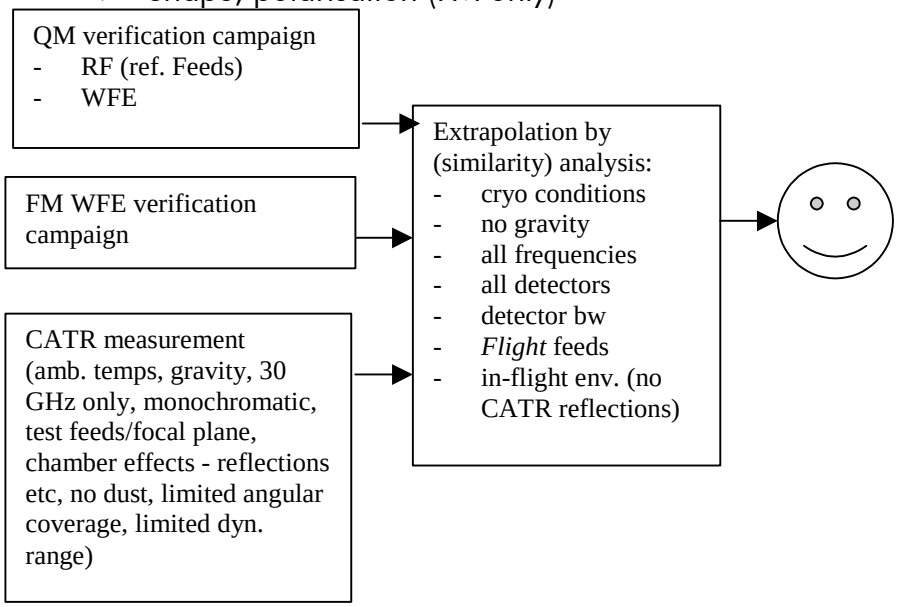

RF sidelobes properties

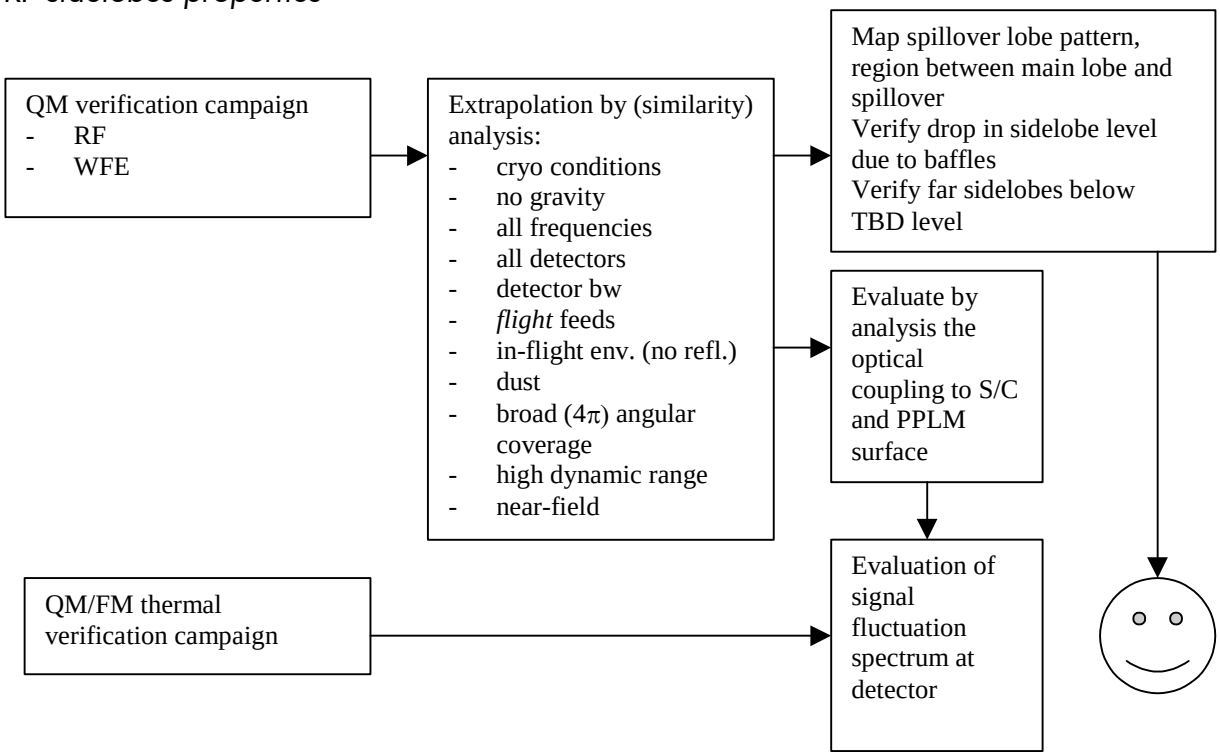

External Straylight

- QM

Verify analysis model by CATR measurement of test piece (Archeops)

CATR measurement of far-field beam shape (amb. temps, gravity, restricted freq., monochromatic, test feeds/focal plane, chamber effects - reflections etc, no dust, limited angular coverage, limited dyn. range)

→ Extrapolation by analysis:
- cryo conditions
- no gravity
- all verify. frequencies
- detector bw
- "reference" feeds
- in-flight env. (no CATR reflections)
- dust
- broad (4π) angular coverage
- high dynamic range

→ Evaluate by analysis the effect of:
- planets
- Sun
- Milky Way

→ Compare to requirements

- FM

QM verification campaign
- RF
- WFE

→ RF/WFE correlation analysis

FM WFE verification campaign

→ Extrapolation by (similarity) analysis:
- cryo conditions
- no gravity
- all frequencies
- detector bw
- "reference" feeds
- in-flight env. (no CATR reflections)
- dust
- broad (4π) angular coverage
- high dynamic range

→ Evaluate by analysis the effect of:
- planets
- Sun
- Milky Way

→ Compare to requirements

Spacecraft Self-Emission

- QM

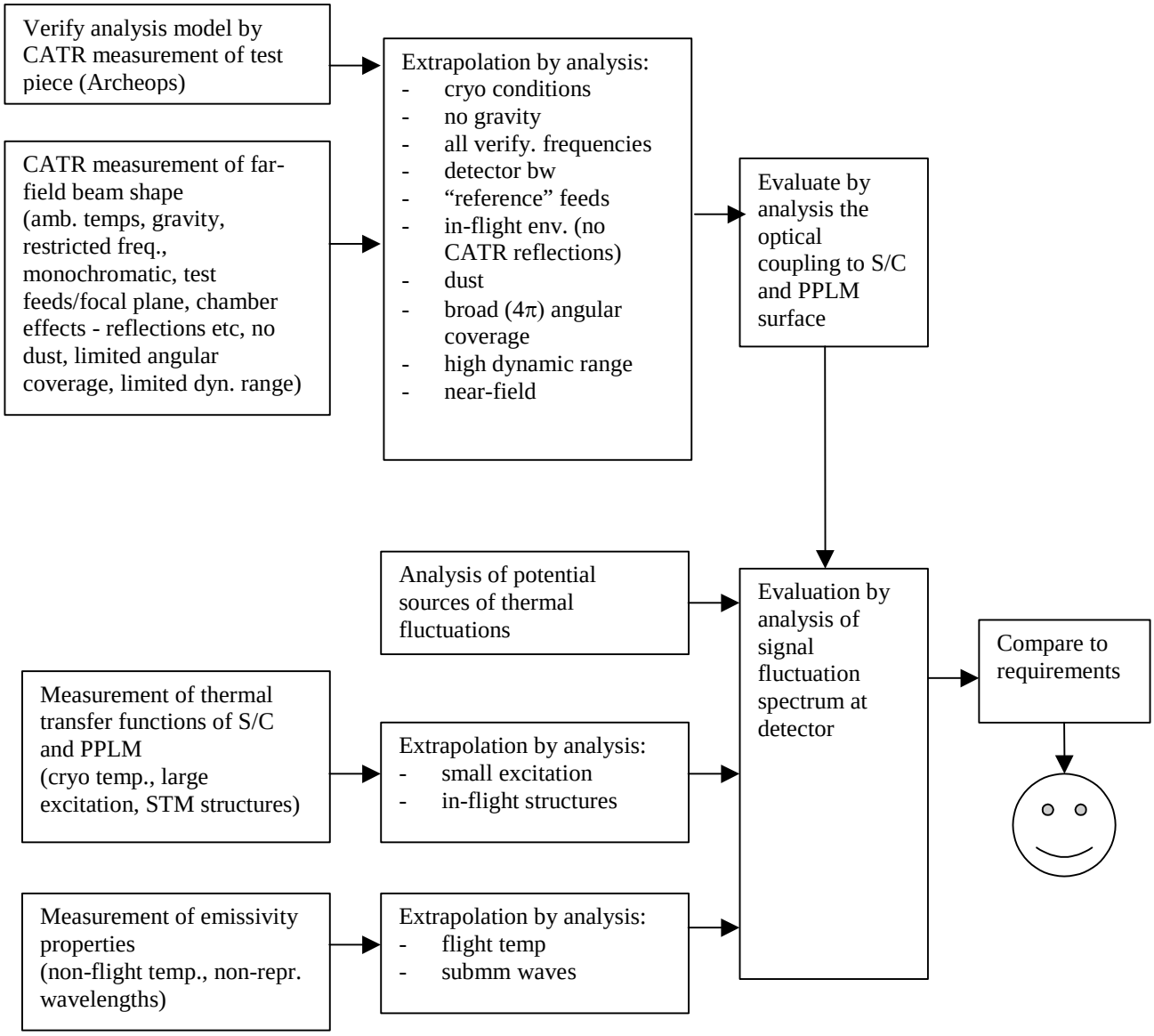

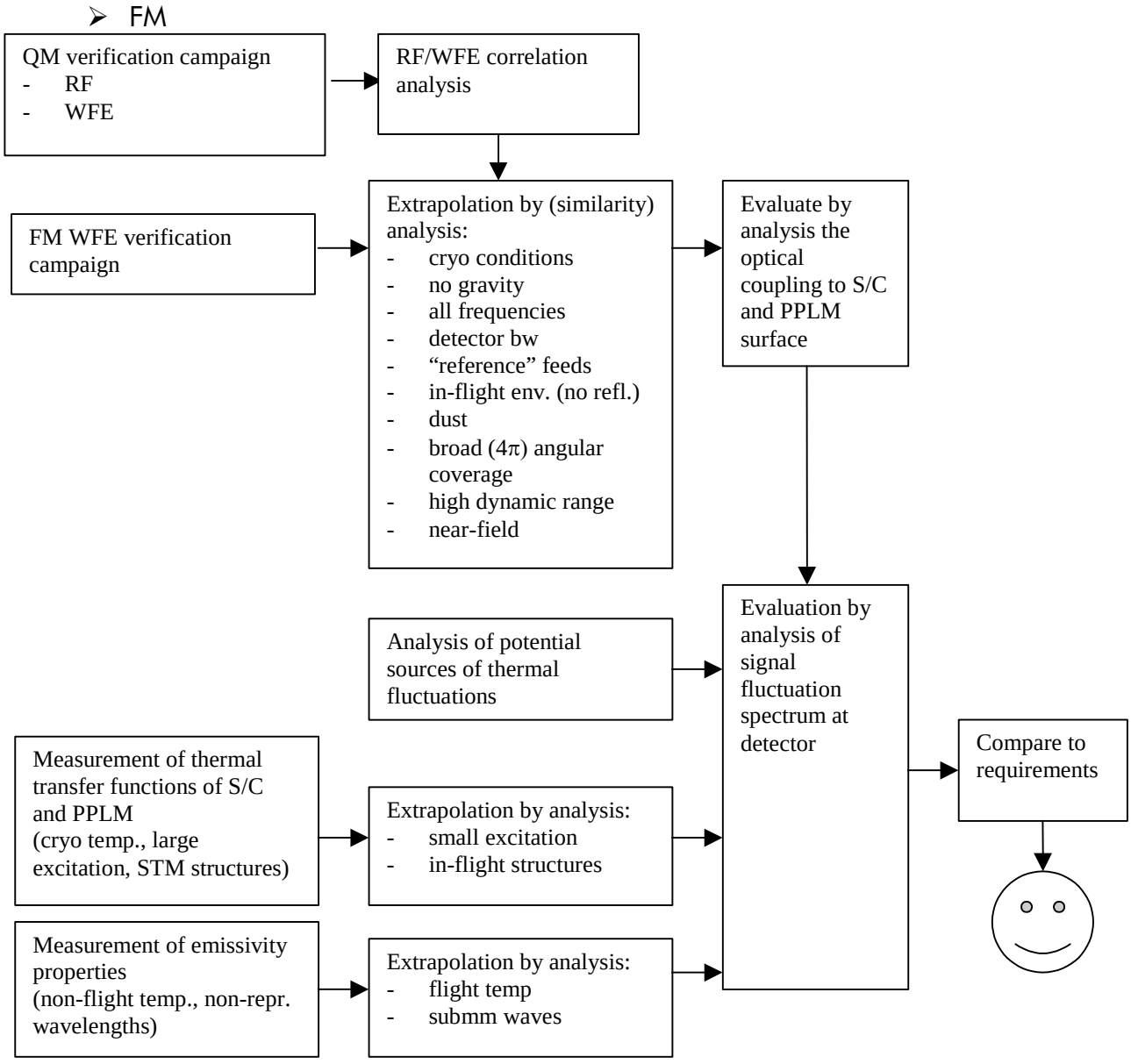

The figure below synthesises the verification flow chart limited to the RF requirements:

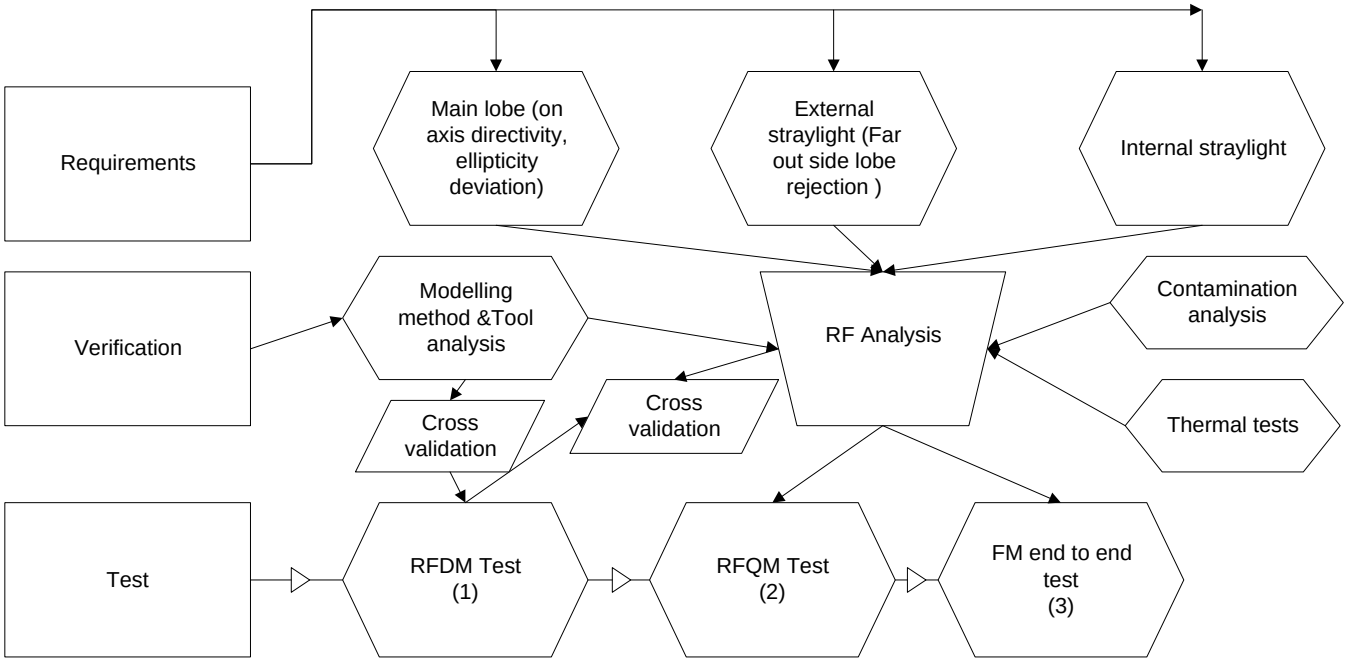

Figure 5-4.1 - RF verification flow chart

FIN DE DOCUMENT
END OF DOCUMENT